

Electronic Supplementary Information

Application of the Boron Center for Design a Covalently Bonded Closely Spaced Triad of Porphyrin-Fullerene Mediated by Dipyromethane

Di Gao, Shawkat M. Aly, Paul-Ludovic Karsenti, Gessie Brisard and Pierre D. Harvey*

Table of Content

Figure S1. Cyclic voltammograms of 6 in DCM, 0.1 M TBAPF ₆ . Scan rate = 100 mV/s.....	3
Figure S2. Cyclic voltammograms of 7 in DCM, 0.1 M TBAPF ₆ . Scan rate = 100 mV/s.....	4
Figure S3. Cyclic voltammograms of 4 in DCM, 0.1 M TBAPF ₆ . Scan rate = 100 mV/s.....	4
Figure S4. Cyclic voltammograms of 5 in DCM, 0.1 M TBAPF ₆ . Scan rate = 100 mV/s.....	4
Figure S5. Cyclic voltammograms of 1 in DCM, 0.1 M TBAPF ₆ . Scan rate = 100 mV/s.....	5
Figure S6. Cyclic voltammograms of 2 in DCM, 0.1 M TBAPF ₆ . Scan rate = 100 mV/s.....	5
Figure S7. Cyclic voltammograms of 8 in DCM, 0.1 M TBAPF ₆ . Scan rate = 100 mV/s.....	6
Figure S8. Cyclic voltammograms of 1-2H in DCM, 0.1 M TBAPF ₆ . Scan rate = 100 mV/s.....	6
Figure S9. Cyclic voltammograms of 9 in DCM, 0.1 M TBAPF ₆ . Scan rate = 100 mV/s.....	7
Figure S10. MO representations after geometry optimization of the frontier MOs for 6 ; energies in eV.....	8
Figure S11. Optimized geometry and percent electronic contributions for 6	9
Figure S12. Bar graph reporting the calculated oscillator strength and calculated position of the 100 st electronic transitions calculated by TDDFT for 6 (bar graph; f = computed oscillator strength). The black line is generated by assigning an arbitrary thickness of 1000 cm ⁻¹ to each bar.....	9
Figure S13. MO representations after geometry optimization of the frontier MOs for 7 ; energies in eV.....	10
Figure S14. Optimized geometry and percent electronic contributions for 7	11
Figure S15. Bar graph reporting the calculated oscillator strength and calculated position of the 100 st electronic transitions calculated by TDDFT for 7 (bar graph; f = computed oscillator strength). The black line is generated by assigning an arbitrary thickness of 1000 cm ⁻¹ to each bar.....	11
Figure S16. Steady-state absorption (black), excitation (blue) and emission (red) of 8 in 2MeTHF at: 1) 77 K and 2) 298 K. Excitation and emission wavelengths are given on the graph.....	12
Figure S17. Steady-state absorption (black), excitation (blue) and emission (red) of 1H2 in 2MeTHF at: 1) 77 K and 2) 298 K. Excitation and emission wavelengths are given on the graph.....	12
Figure S18. Steady-state absorption (black), excitation (blue) and emission (red) of 1 in 2MeTHF at: 1) 77 K and 2) 298 K. Excitation and emission wavelengths are given on the graph.....	13
Figure S19. Steady-state measurements absorption (black), excitation (blue) and emission (red) in 2MeTHF at 77 K; wavelengths used to measure the emission and excitation spectra are given on the graph.....	13
Figure S20. Time-resolved fluorescence of: 1) 4 and 2) 5 in 2MeTHF at 298 K monitored by Streak camera after excitation at 490 nm with a 100 fs laser.....	14
Figure S21. Kinetic traces of fluorescence signals in 2MeTHF at 77 K as collected from Streak camera (λ_{ex} = 490 nm, FWHM of laser pulse ~ 100 fs; IRF ~ 8ps).	14
Figure S22. fs-TA spectra (left, delay time given on graph) and kinetic profile (right, monitoring wavelengths given on	

graph) of dyad 5 in 2MeTHF at 298 K. TA spectra collected using ~90 fs laser excitation at 520 nm.....	15
Figure S23. fs-TA spectra of 6 (1) and kinetics monitored for 4 and 6 at 440 nm (2) in 2MeTHF at 298 K; $\lambda_{\text{ex}} = 520$ nm (laser pulse ~90 fs).	15
Figure S24. fs-TA of 6 : 1)spectra at different delay time and 2) kinetics monitored at 1010 nm (inset showing rising of the signal) in 2MeTHF at 298 K; $\lambda_{\text{ex}} = 520$ nm (laser pulse ~90 fs).	15
Figure S25. Kinetic traces of TAS signals in 2MeTHF at 298 K for 4 and 6 ($\lambda_{\text{ex}}= 520$ nm, FWHM of laser pulse ~ 90 fs).	16
Figure S26. fs-TA spectra of 7 (1) and kinetics monitored for 5 and 7 at 425 nm (2) in 2MeTHF at 298 K; $\lambda_{\text{ex}} = 520$ nm (laser pulse ~90 fs).	16
Figure S27. fs-TA of 7 : 1)spectra at different delay time and 2) kinetics monitored at 1010 nm (inset showing rising of the signal) in 2MeTHF at 298 K; $\lambda_{\text{ex}} = 520$ nm (laser pulse ~90 fs).	17
Figure S28. Kinetic traces of TAS signals in 2MeTHF at 298 K for 5 and 7 ($\lambda_{\text{ex}}= 520$ nm, FWHM of laser pulse ~ 90 fs).	17
Figure S29. ^1H NMR spectra of 8 in CDCl_3	18
Figure S30. ^1H NMR spectra of 9 in CDCl_3	18
Figure S31. ^1H NMR spectra of 3 in CDCl_3	19
Figure S32. ^1H NMR spectra of 3 in CDCl_3	19
Figure S33. ^1H NMR spectra of 4 in CDCl_3	20
Figure S34. ^1H NMR spectra of 5 in CDCl_3	20
Figure S35. ^1H NMR spectra of 6 in CDCl_3	21
Figure S36. ^1H NMR spectra of 7 in CDCl_3	21
Figure S37. MALDI-TOF spectra of 8	22
Figure S38. MALDI-TOF spectra of 9	22
Figure S39. MALDI-TOF spectra of 3	23
Figure S40. MALDI-TOF spectra of 4	23
Figure S41. MALDI-TOF spectra of 5	24
Figure S42. MALDI-TOF spectra of 6	24
Figure S43. MALDI-TOF spectra of 7	25
 Table S1. Calculated position, oscillator strength (f) and major contributions of the first 100 singlet-singlet electronic transitions for 6	26
Table S2. Calculated position, oscillator strength (f) and major contributions of the first 100 singlet-singlet electronic transitions for 7	29

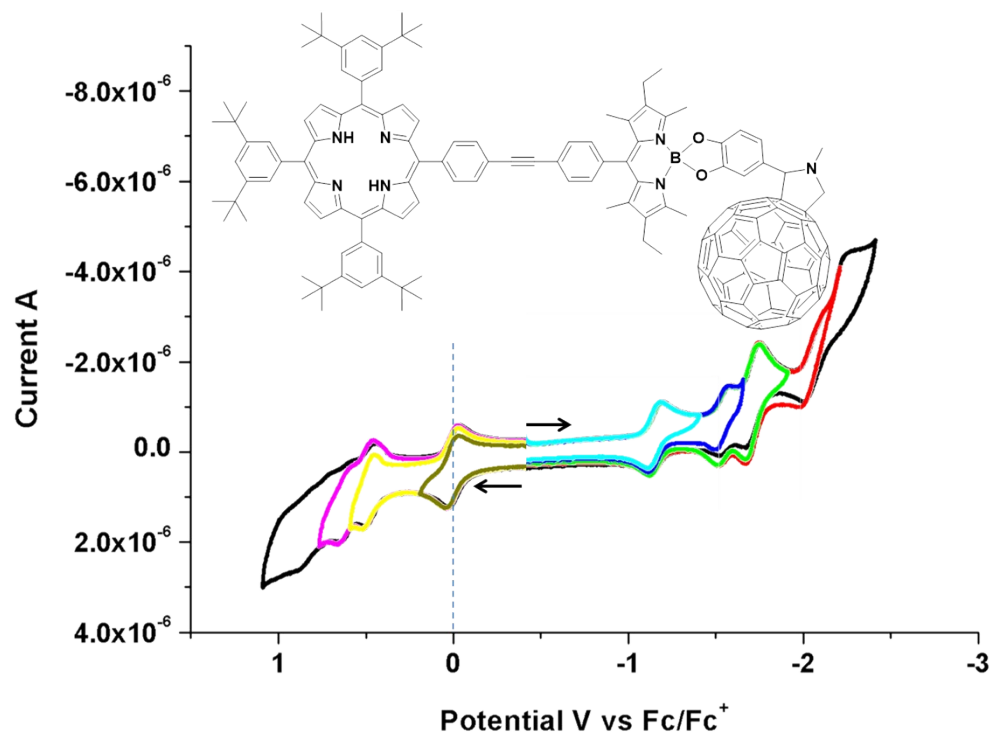


Figure S1. Cyclic voltammograms of **6** in DCM, 0.1 M TBAPF₆. Scan rate = 100 mV/s.

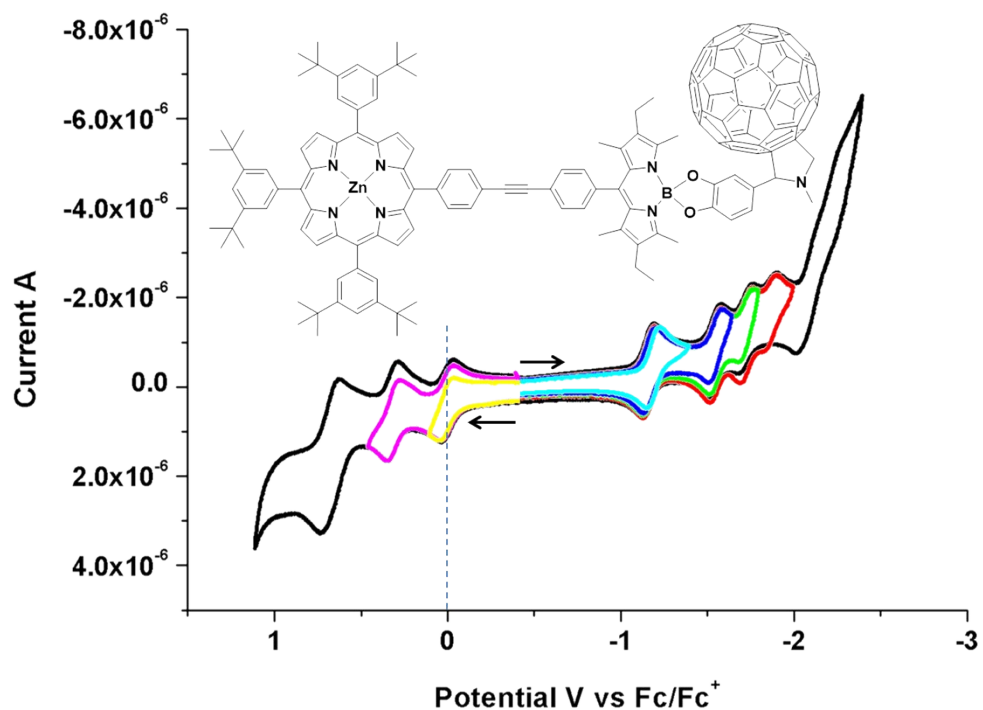


Figure S2. Cyclic voltammograms of **7** in DCM, 0.1 M TBAPF₆. Scan rate = 100 mV/s.

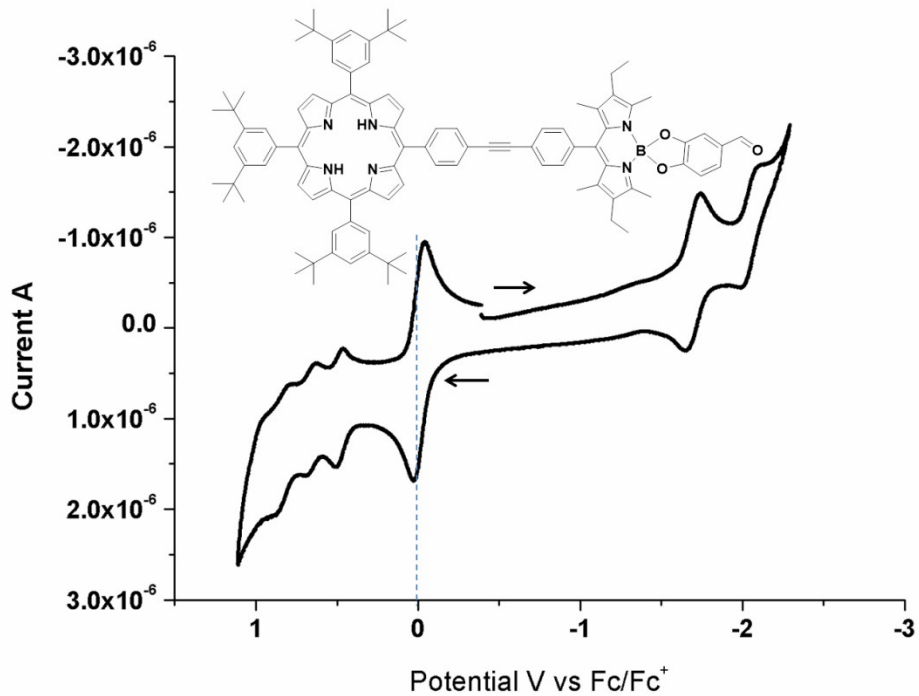


Figure S3. Cyclic voltammograms of **4** in DCM, 0.1 M TBAPF₆. Scan rate = 100 mV/s.

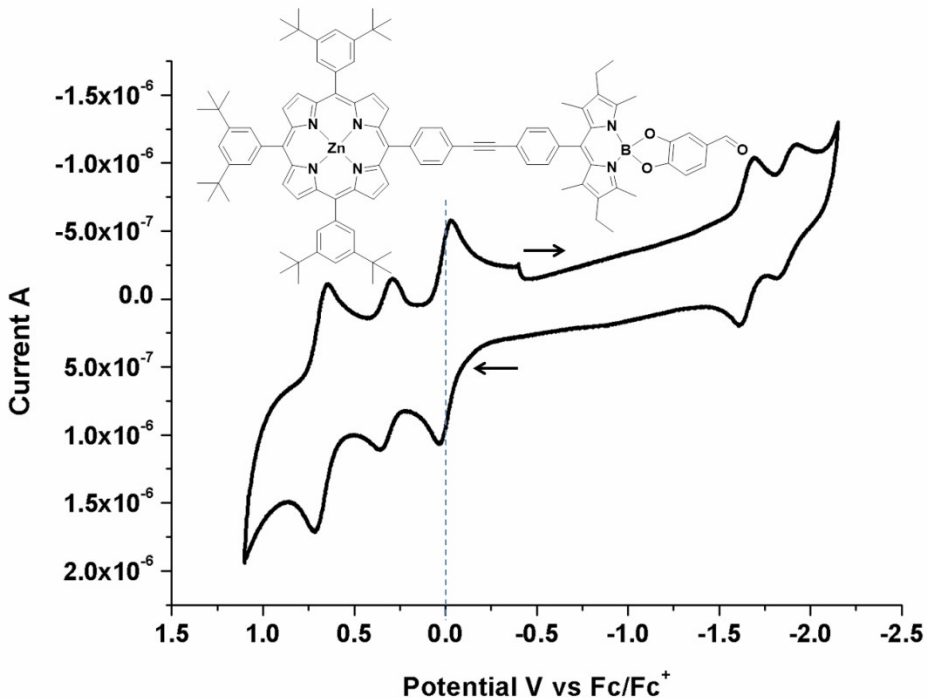


Figure S4. Cyclic voltammograms of **5** in DCM, 0.1 M TBAPF₆. Scan rate = 100 mV/s.

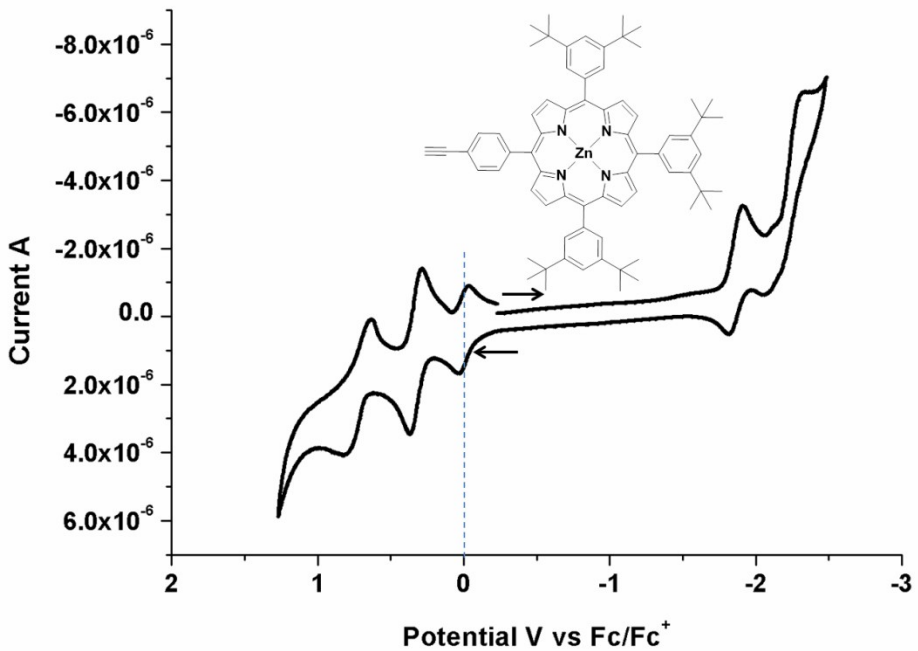


Figure S5. Cyclic voltammograms of **1** in DCM, 0.1 M TBAPF₆. Scan rate = 100 mV/s.

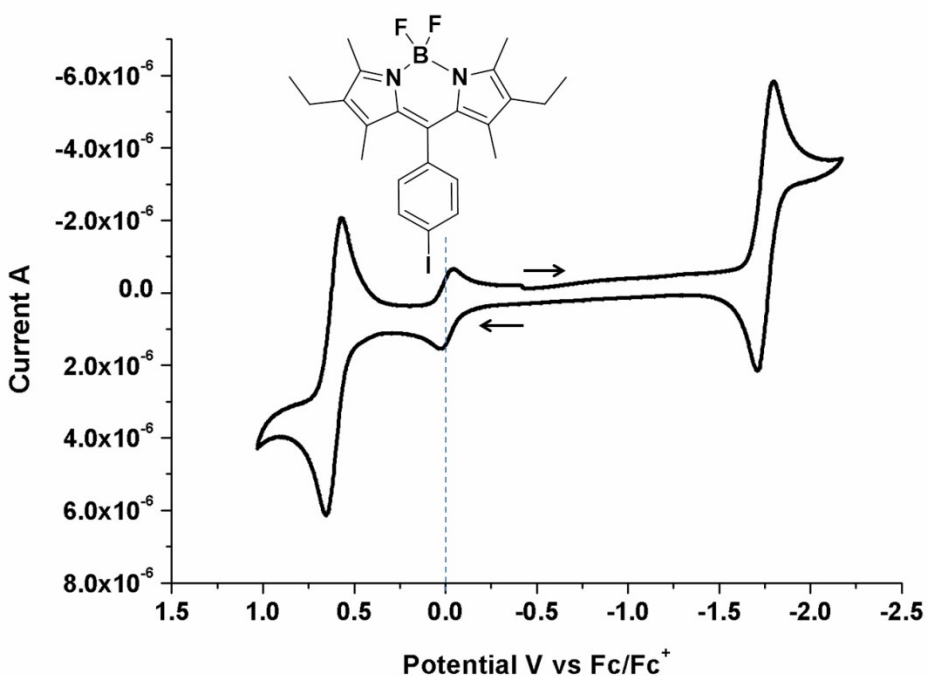


Figure S6. Cyclic voltammograms of **2** in DCM, 0.1 M TBAPF₆. Scan rate = 100 mV/s.

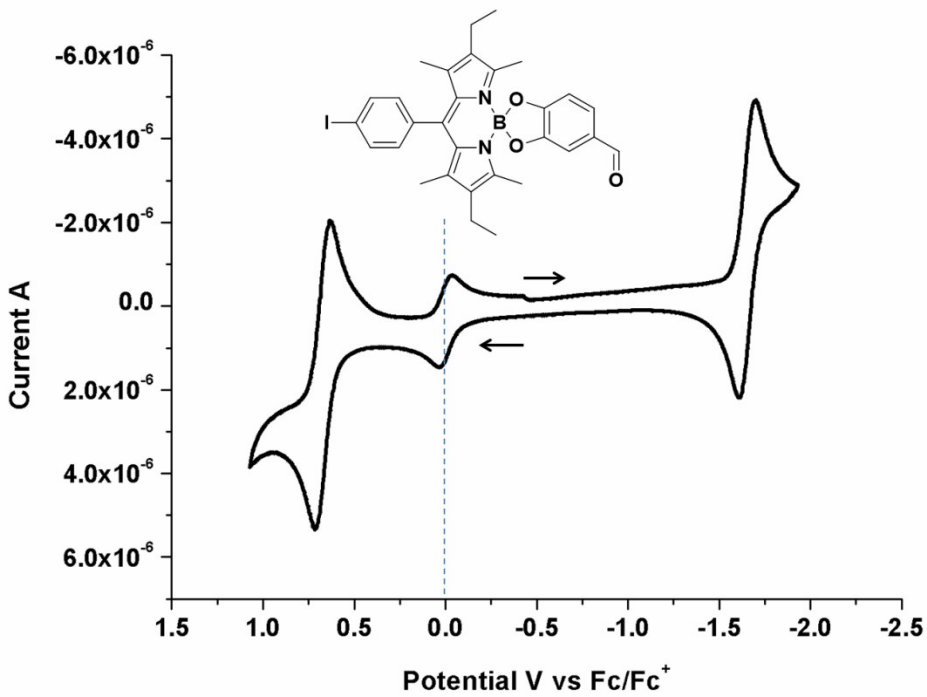


Figure S7. Cyclic voltammograms of **8** in DCM, 0.1 M TBAPF₆. Scan rate = 100 mV/s.

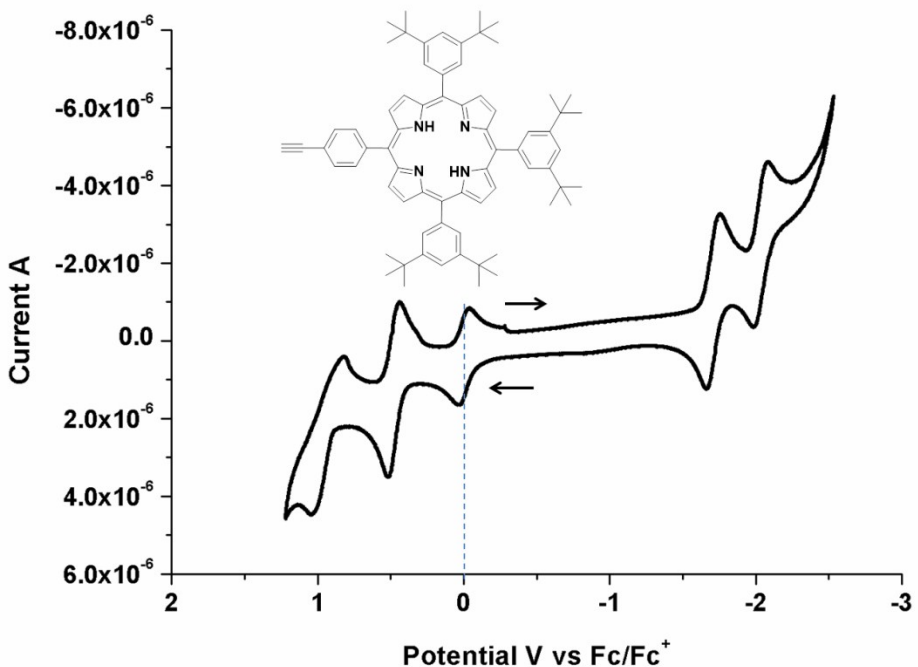


Figure S8. Cyclic voltammograms of **1-2H** in DCM, 0.1 M TBAPF₆. Scan rate = 100 mV/s.

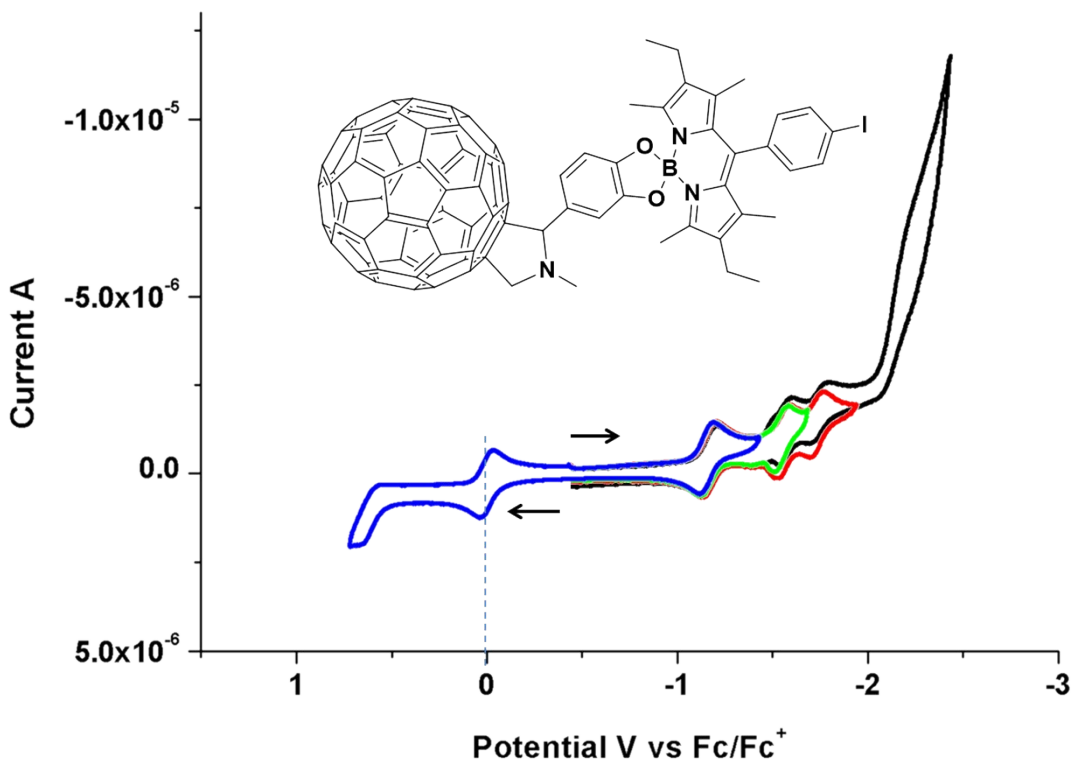


Figure S9. Cyclic voltammograms of **9** in DCM, 0.1 M TBAPF₆. Scan rate = 100 mV/s.

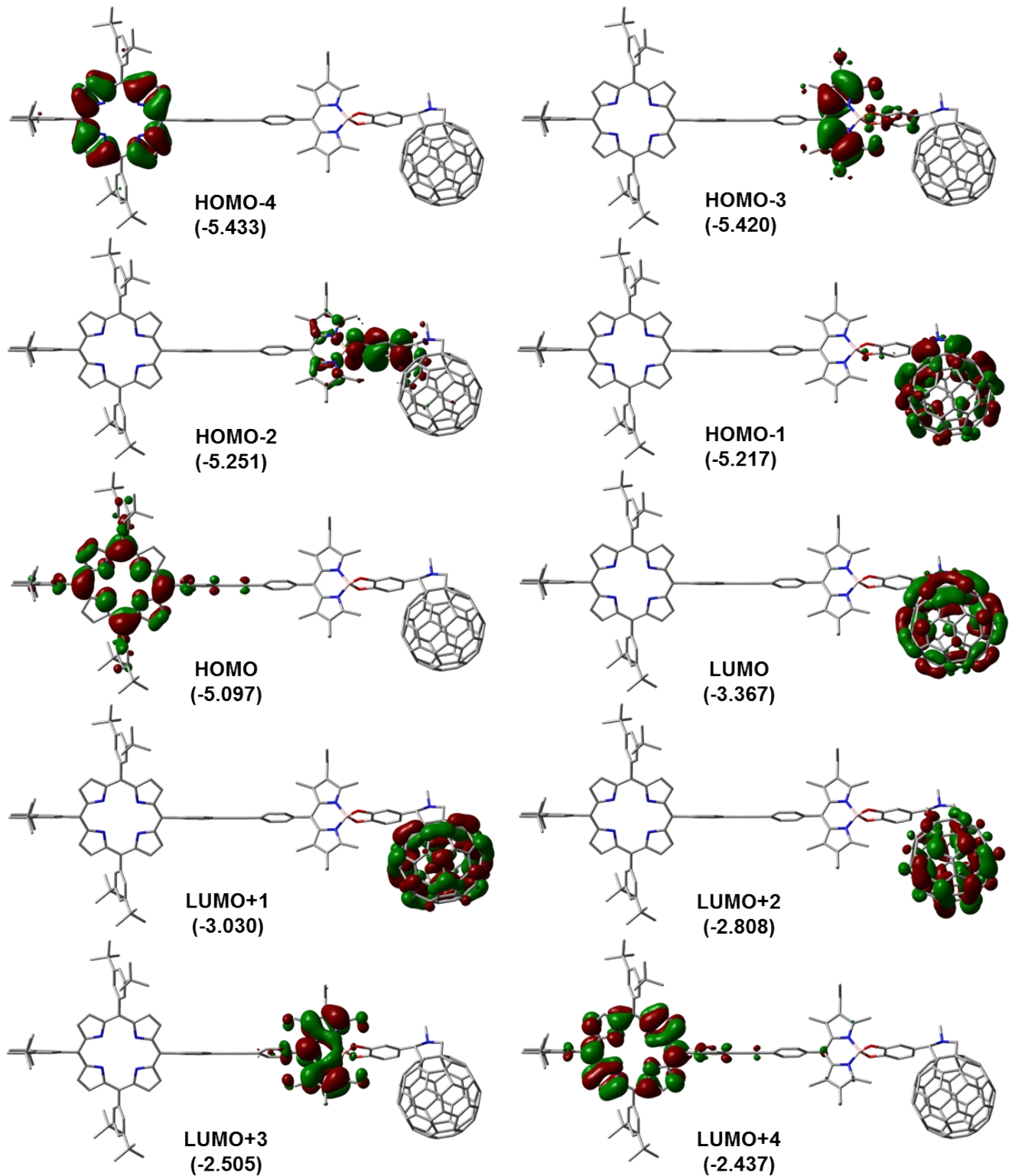
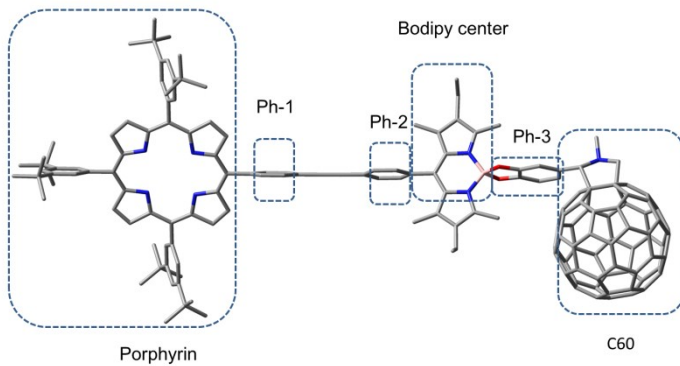


Figure S10. MO representations after geometry optimization of the frontier MOs for **6**; energies in eV.



	MO									
	H-4	H-3	H-2	H-1	HOMO	LUMO	L+1	L+2	L+3	L+4
Porphyrin	98.5	0	0	0	93.8	0	0	0	1.71	91.70
Bodipy - Center	0	93.20	16.40	0.55	0.08	1.07	0.09	0.29	89.40	2.05
Ph-1	1.48	0	0	0	5.04	0	0	0	0.42	5.05
Ph-2	0.02	0.33	0.03	0	1.07	0	0	0	7.23	1.17
Ph-3	0	5.55	72.40	1.54	0	0.66	0.36	0.16	1.18	0.03
C60	0	0.93	11.20	97.9	0	98.30	99.60	99.50	0.04	0

Figure S11. Optimized geometry and percent electronic contributions for **6**

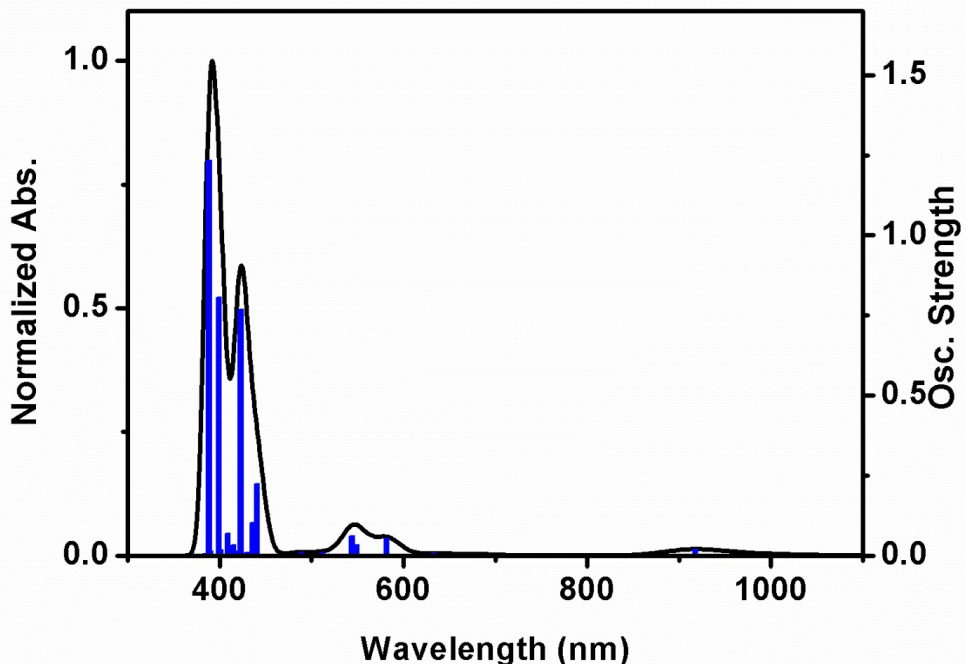


Figure S12. Bar graph reporting the calculated oscillator strength and calculated position of the 100th electronic transitions calculated by TDDFT for **6** (bar graph; f = computed oscillator strength). The black line is generated by assigning an arbitrary thickness of 1000 cm⁻¹ to each bar.

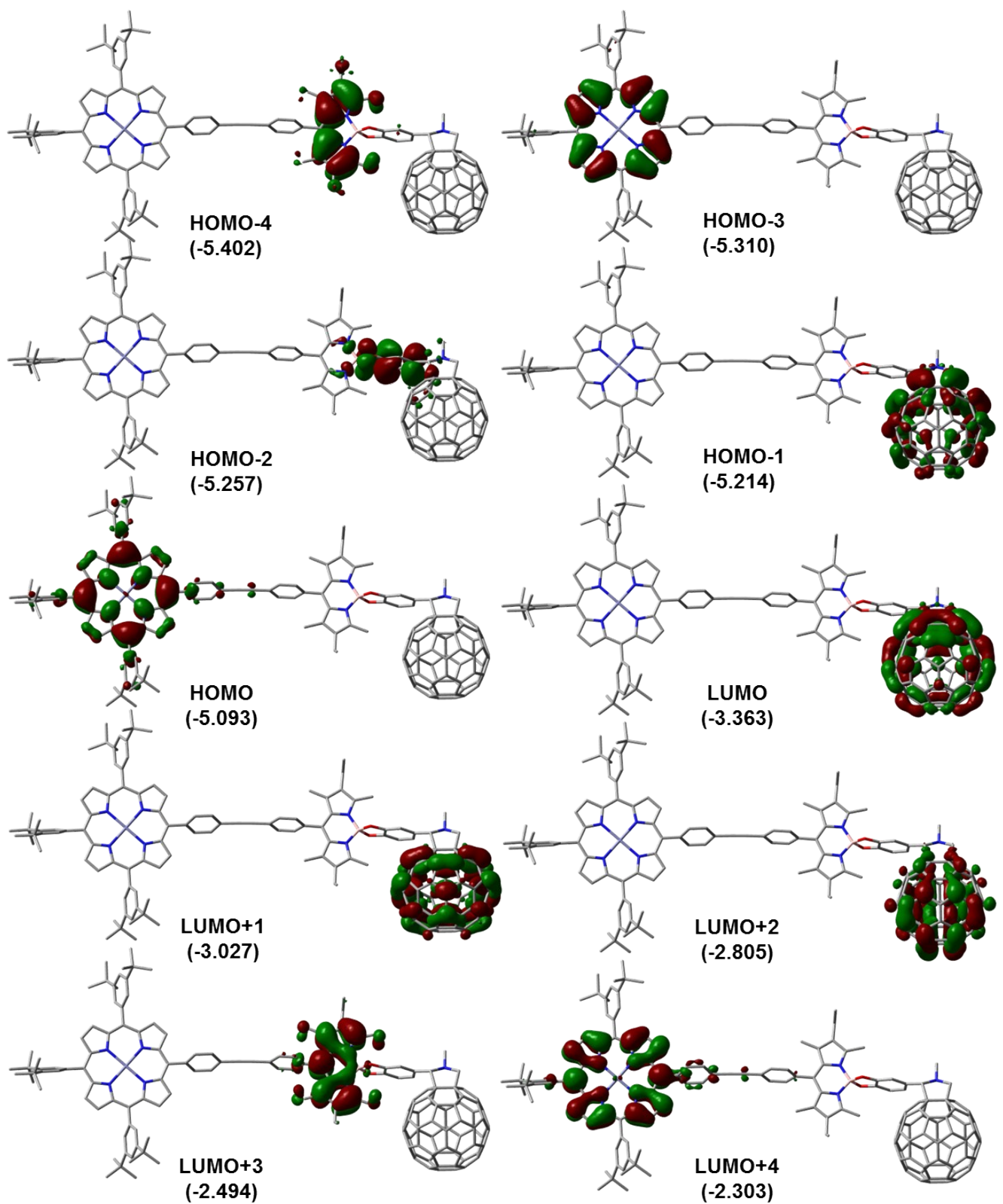
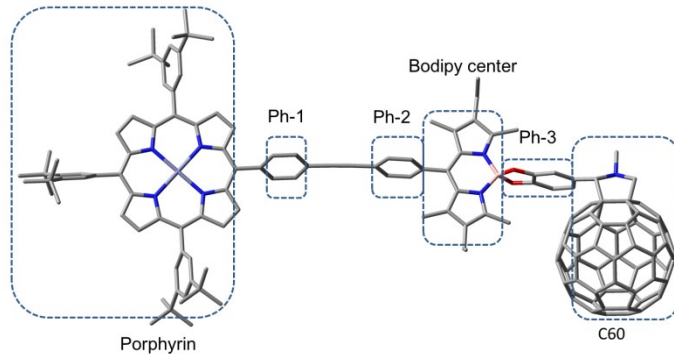


Figure S13. MO representations after geometry optimization of the frontier MOs for **7**; energies in eV.



	MO									
	H-4	H-3	H-2	H-1	HOMO	LUMO	L+1	L+2	L+3	L+4
Porphyrin	0	98.8	0	0	94.3	0	0	0	0.12	92.80
Bodipy - Center	98.6	0	12.30	0.34	0.07	1.02	0.11	0.52	91.30	0.31
Ph-1	0	1.21	0	0	4.70	0	0	0	0.17	5.66
Ph-2	0.27	0	0	0	0.88	0	0	0	7.06	1.22
Ph-3	0.93	0	76.80	0.53	0	0.71	0.37	0.16	1.22	0
C60	0.24	0	10.80	99.10	0	98.30	99.60	99.50	0.09	0

Figure S14. Optimized geometry and percent electronic contributions for **7**

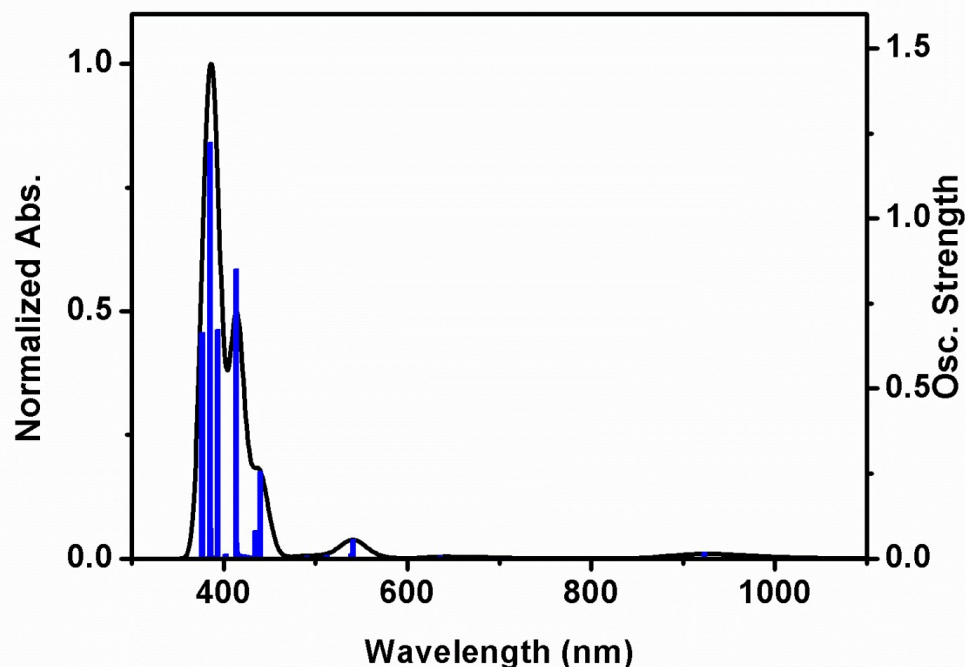


Figure S15. Bar graph reporting the calculated oscillator strength and calculated position of the 100th electronic transitions calculated by TDDFT for **7** (bar graph; f = computed oscillator strength). The black line is generated by assigning an arbitrary thickness of 1000 cm⁻¹ to each bar.

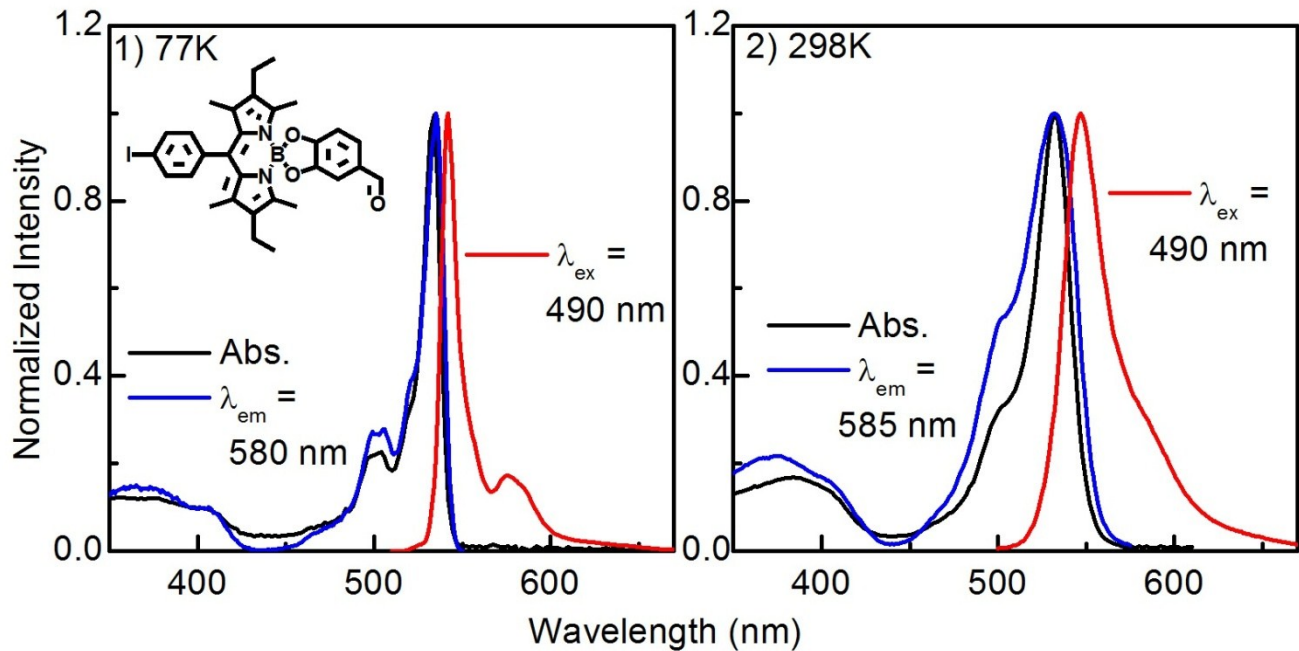


Figure S16. Steady-state absorption (black), excitation (blue) and emission (red) of **8** in 2MeTHF at: 1) 77 K and 2) 298 K. Excitation and emission wavelengths are given on the graph.

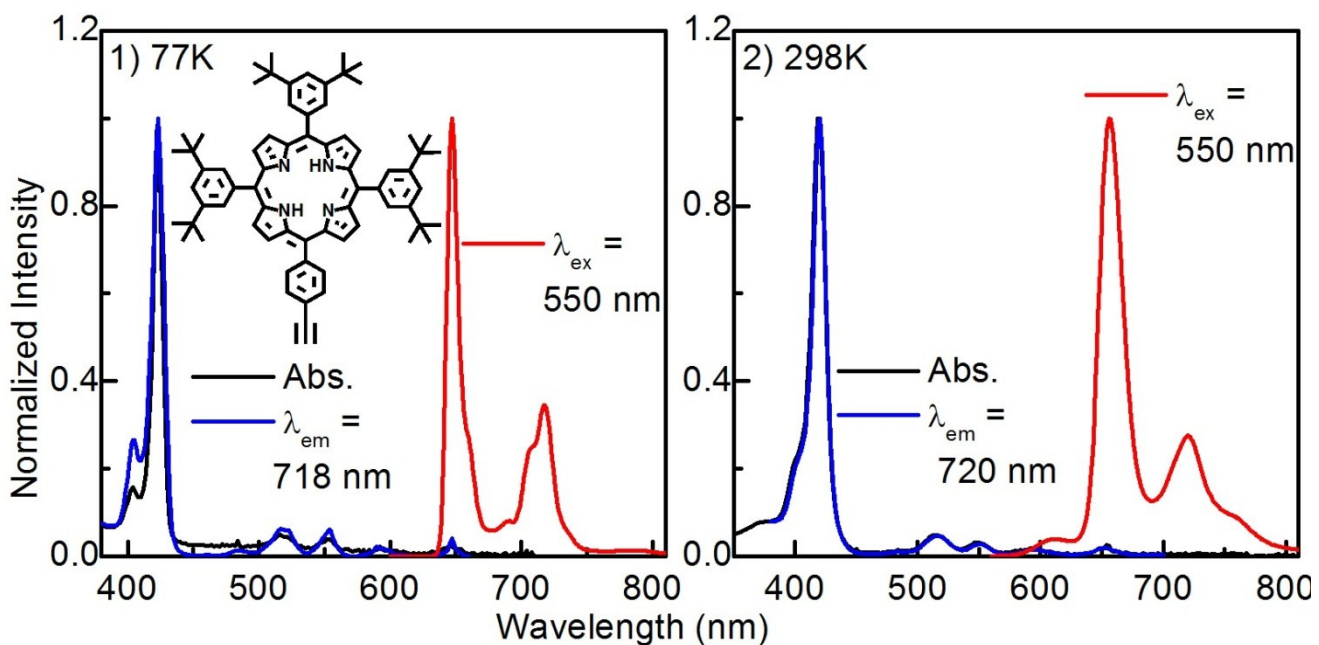


Figure S17. Steady-state absorption (black), excitation (blue) and emission (red) of **1H2** in 2MeTHF at: 1) 77 K and 2) 298 K. Excitation and emission wavelengths are given on the graph.

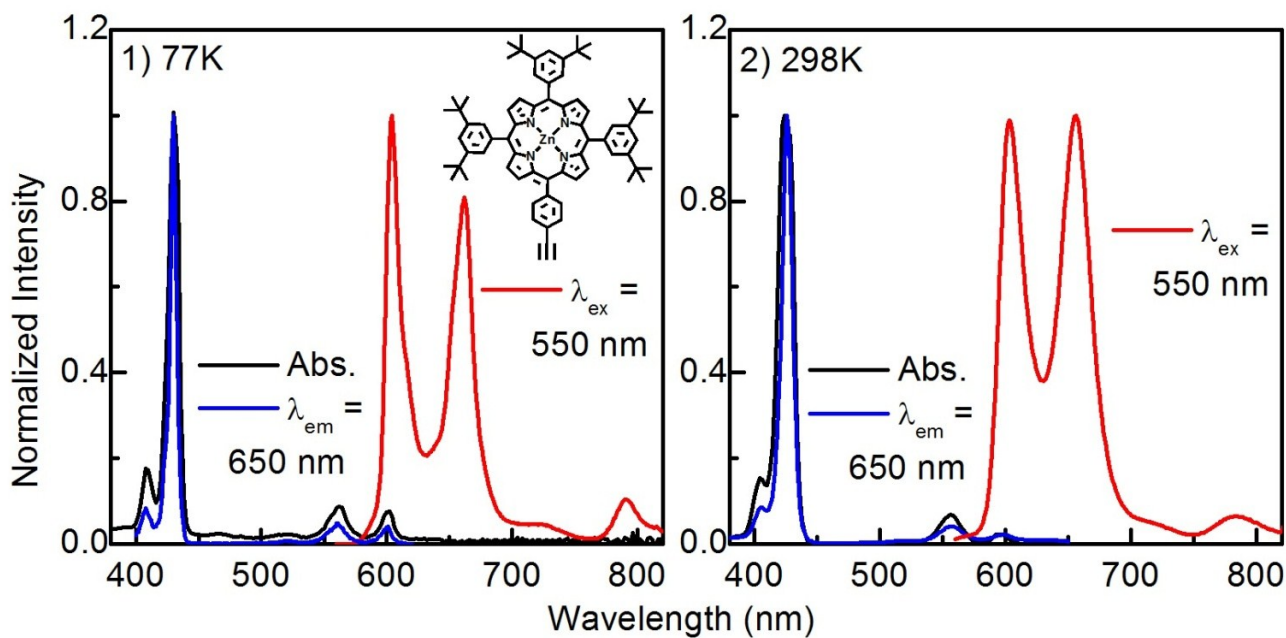


Figure S18. Steady-state absorption (black), excitation (blue) and emission (red) of **1** in 2MeTHF at: 1) 77 K and 2) 298 K. Excitation and emission wavelengths are given on the graph.

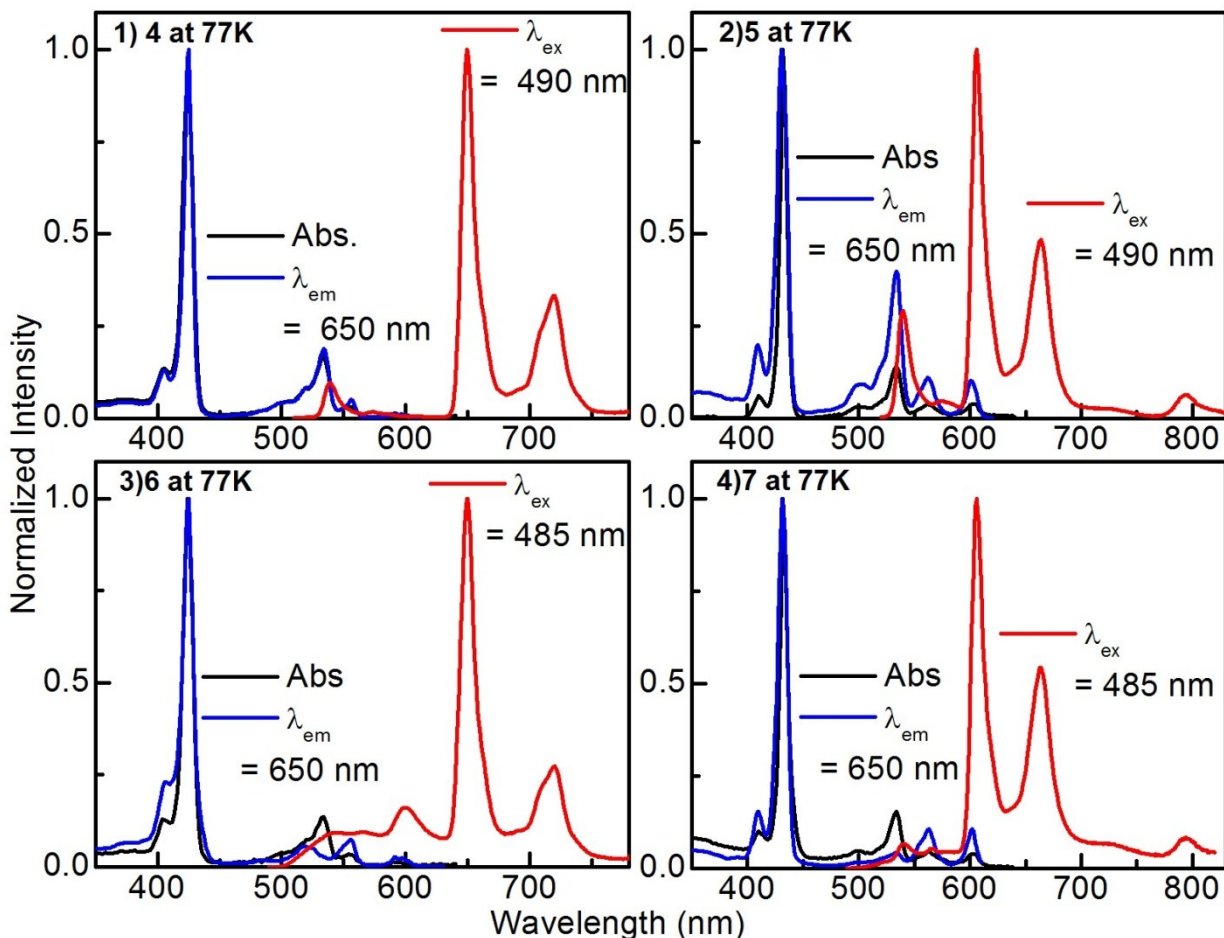


Figure S19. Steady-state measurements absorption (black), excitation (blue) and emission (red) in 2MeTHF at 77 K; wavelengths used to measure the emission and excitation spectra are given on the graph.

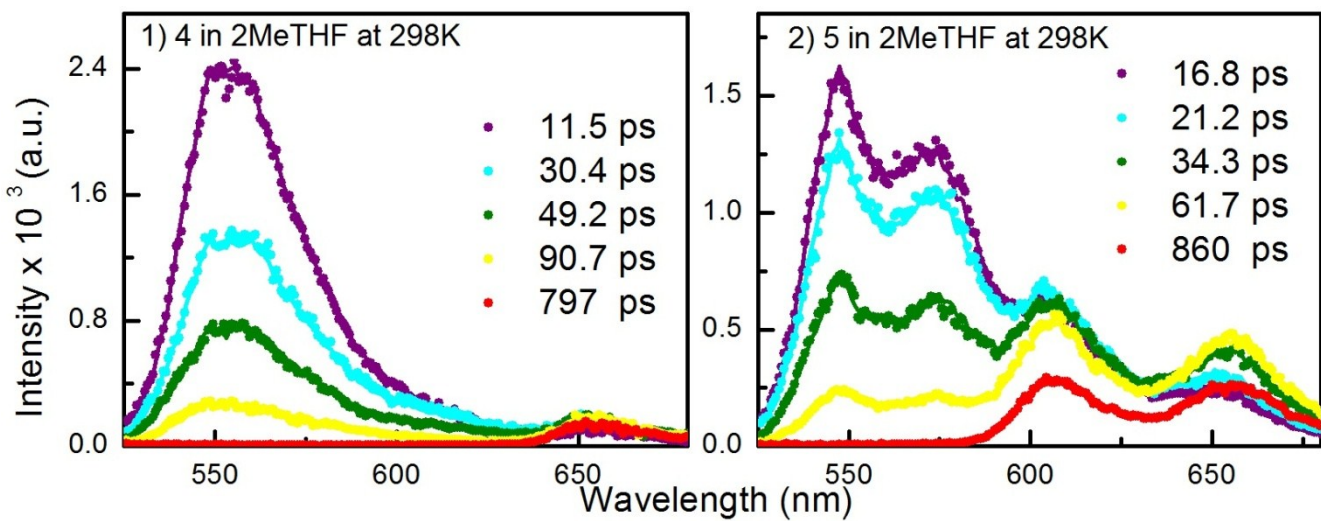


Figure S20. Time-resolved fluorescence of: 1) **4** and 2) **5** in 2MeTHF at 298 K monitored by Streak camera after excitation at 490 nm with a 100 fs laser.

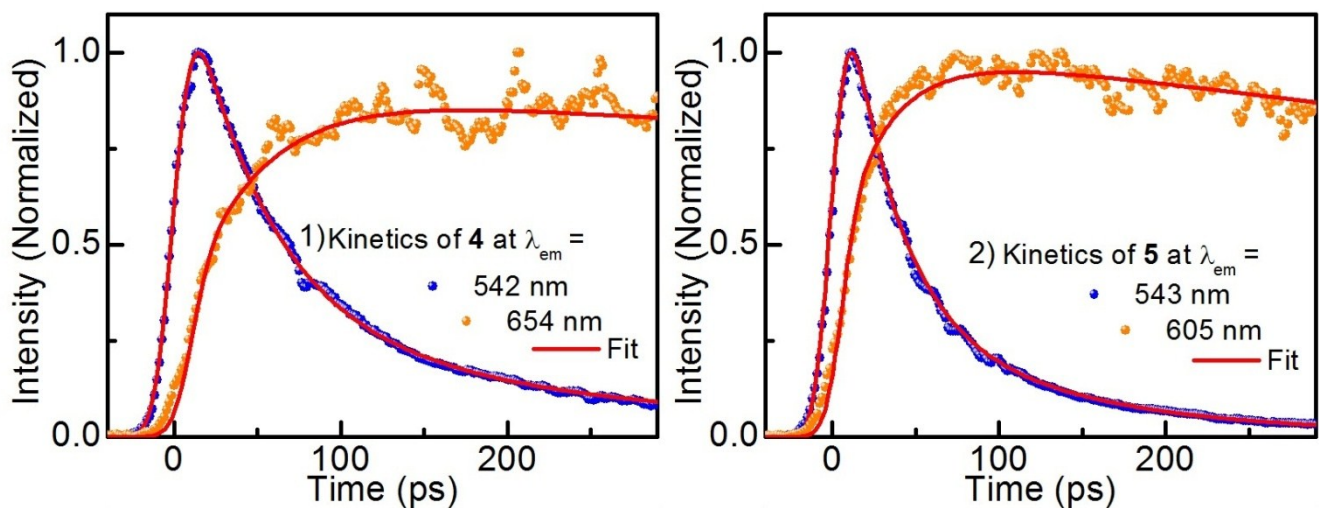


Figure S21. Kinetic traces of fluorescence signals in 2MeTHF at 77 K as collected from Streak camera ($\lambda_{\text{ex}} = 490$ nm, FWHM of laser pulse ~ 100 fs; IRF ~ 8 ps).

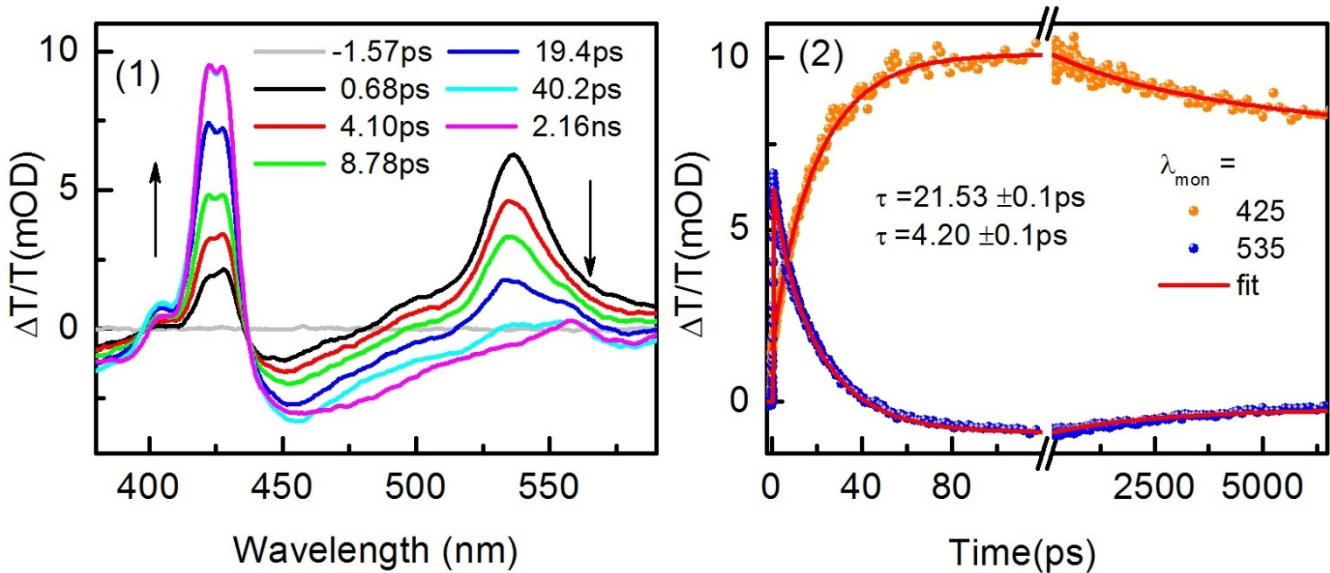


Figure S22. fs-TA spectra (left, delay time given on graph) and kinetic profile (right, monitoring wavelengths given on graph) of dyad **5** in 2MeTHF at 298 K. TA spectra collected using ~90 fs laser excitation at 520 nm.

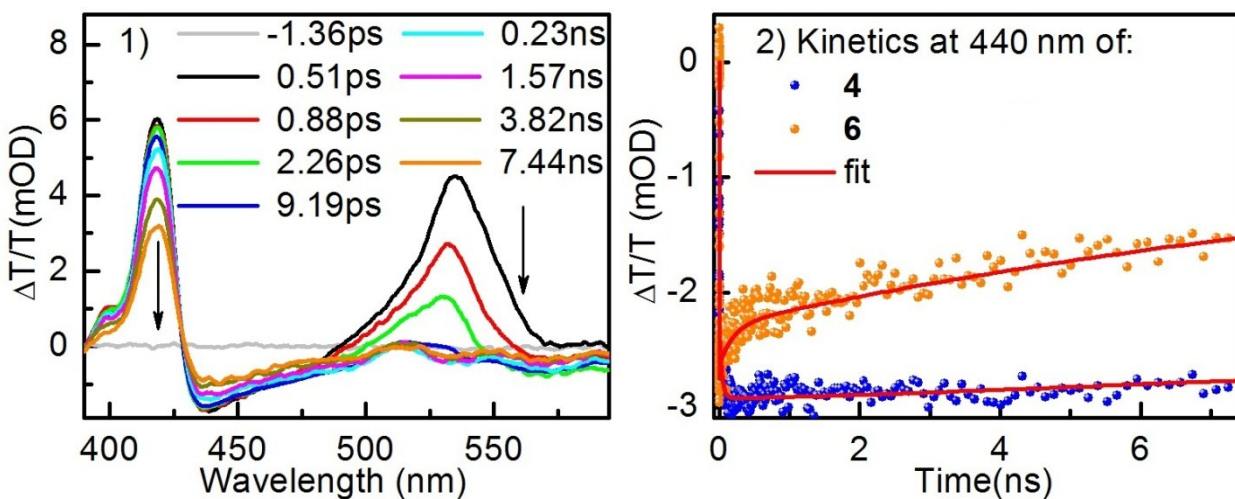


Figure S23. fs-TA spectra of **6** (1) and kinetics monitored for **4** and **6** at 440 nm (2) in 2MeTHF at 298 K; $\lambda_{\text{ex}} = 520$ nm (laser pulse ~90 fs).

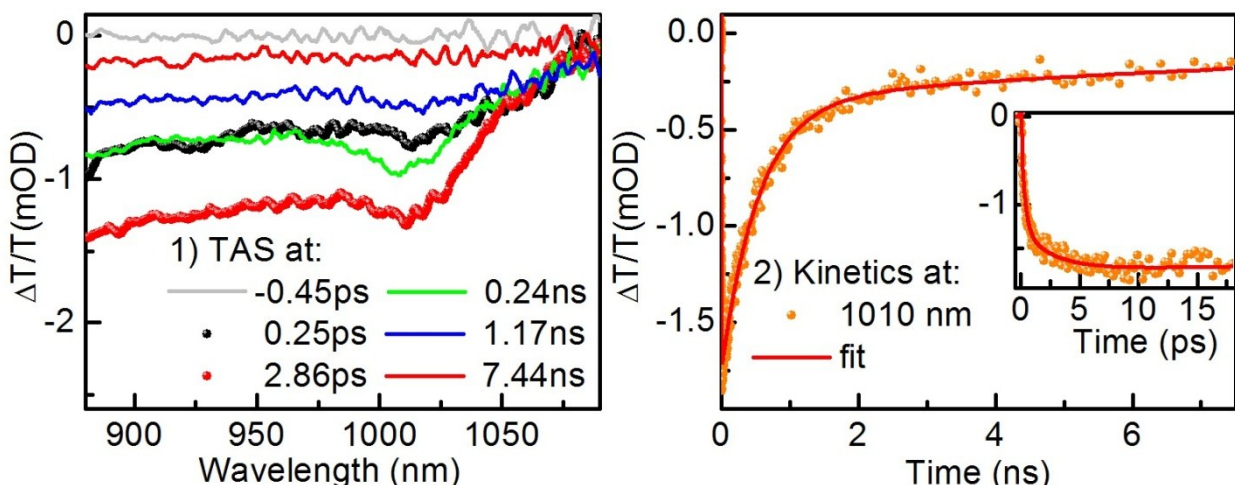


Figure S24. fs-TA of **6**: 1)spectra at different delay time and 2) kinetics monitored at 1010 nm (inset showing rising of the signal) in 2MeTHF at 298 K; $\lambda_{\text{ex}} = 520$ nm (laser pulse ~90 fs).

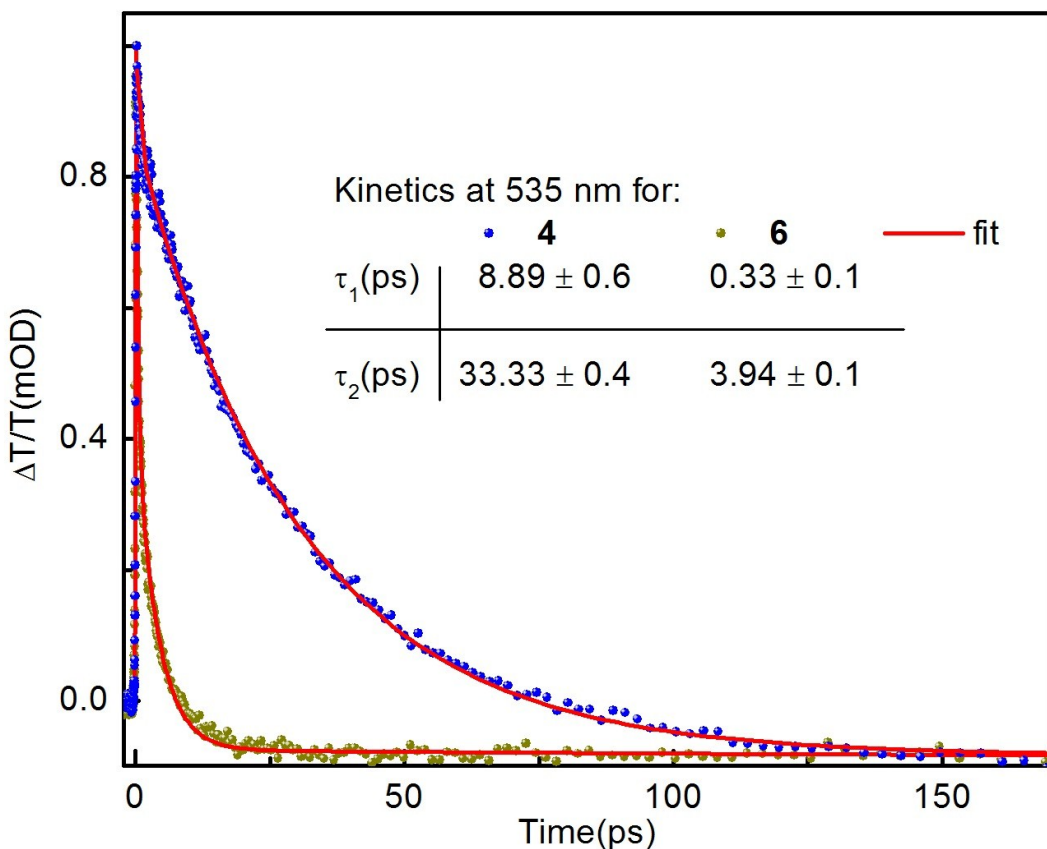


Figure S25. Kinetic traces of TAS signals in 2MeTHF at 298 K for **4** and **6** ($\lambda_{\text{ex}} = 520$ nm, FWHM of laser pulse ~ 90 fs).

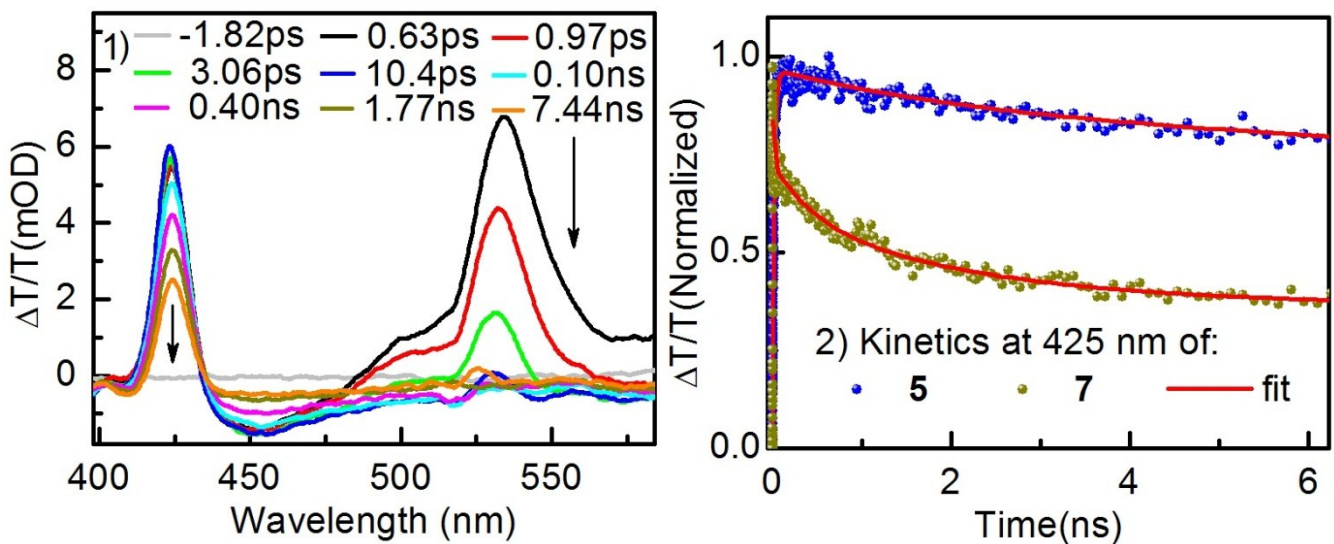


Figure S26. fs-TA spectra of **7** (1) and kinetics monitored for **5** and **7** at 425 nm (2) in 2MeTHF at 298 K; $\lambda_{\text{ex}} = 520$ nm (laser pulse ~ 90 fs).

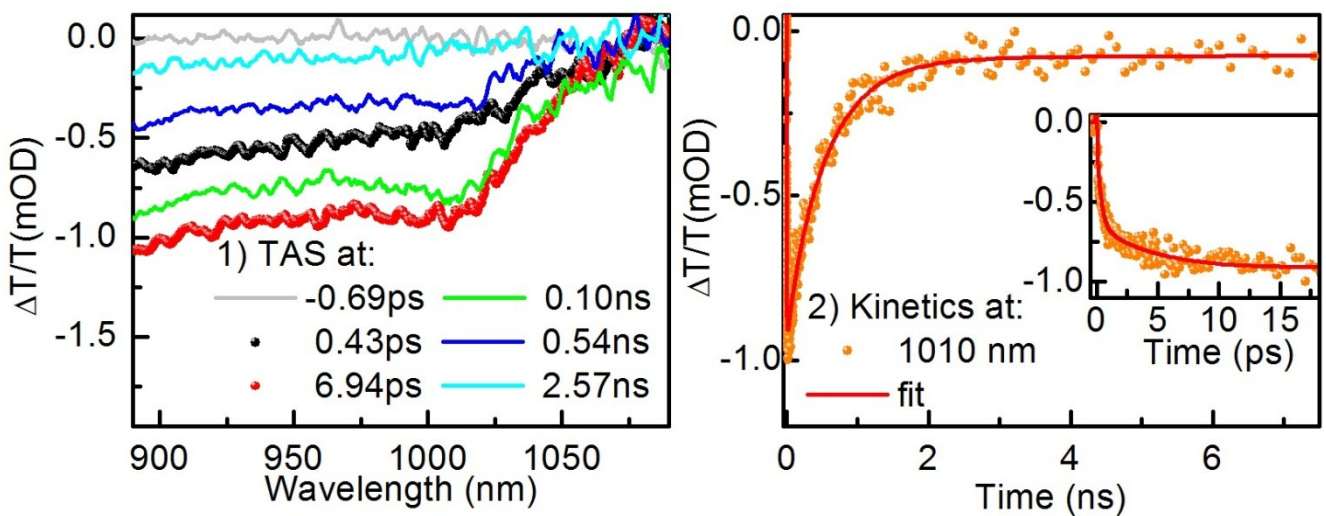


Figure S27. fs-TA of **7**: 1) spectra at different delay time and 2) kinetics monitored at 1010 nm (inset showing rising of the signal) in 2MeTHF at 298 K; $\lambda_{\text{ex}} = 520$ nm (laser pulse ~ 90 fs).

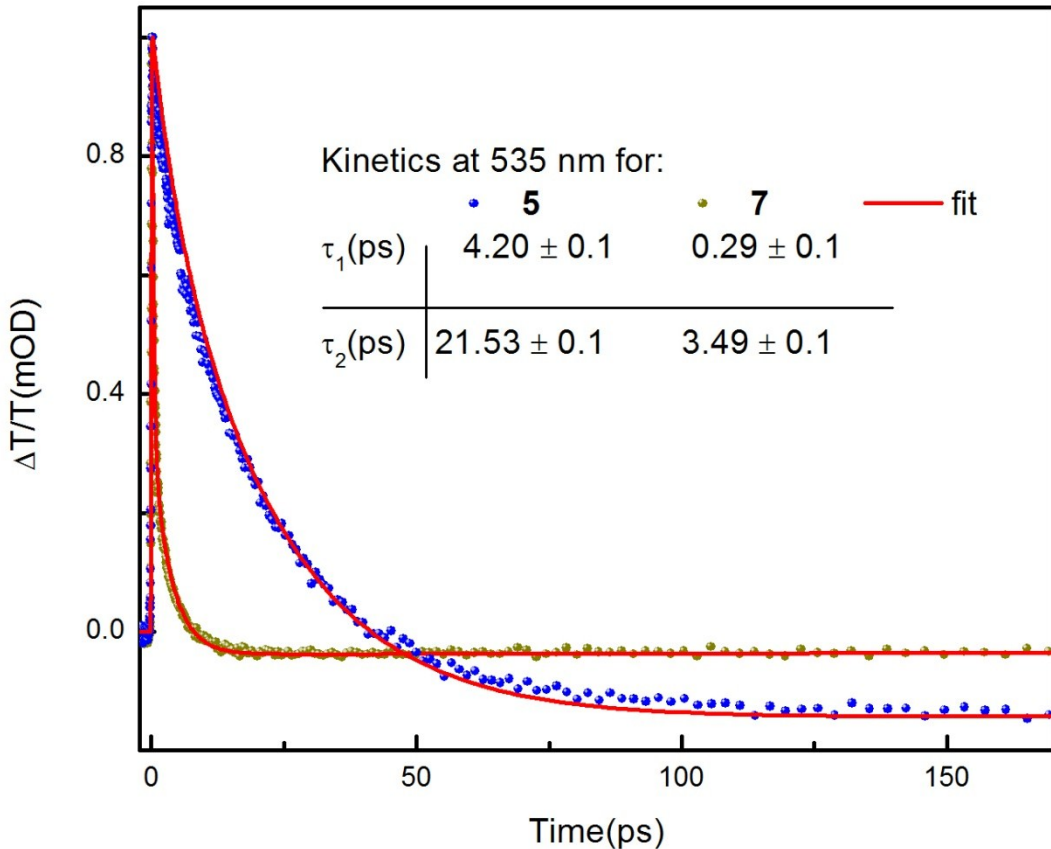


Figure S28. Kinetic traces of TAS signals in 2MeTHF at 298 K for **5** and **7** ($\lambda_{\text{ex}} = 520$ nm, FWHM of laser pulse ~ 90 fs).

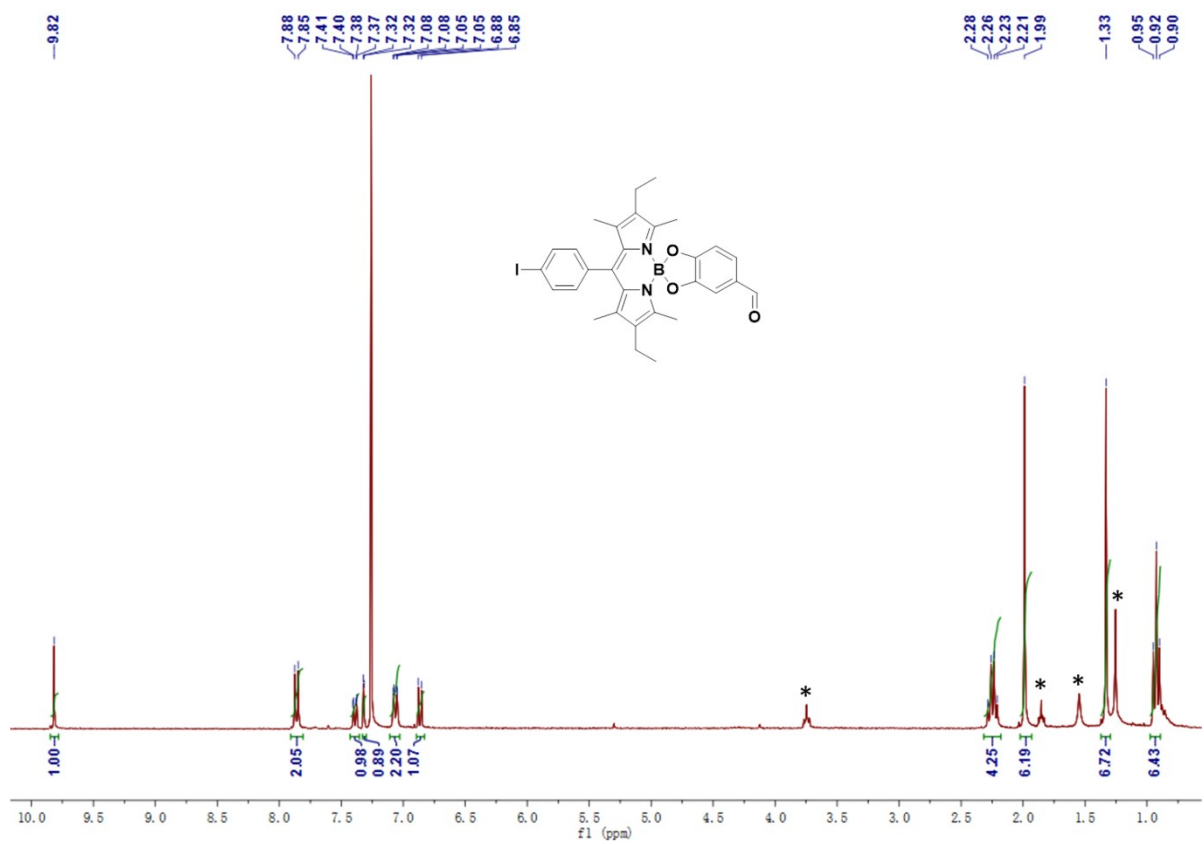


Figure S29. ^1H NMR spectra of **8** in CDCl_3 .

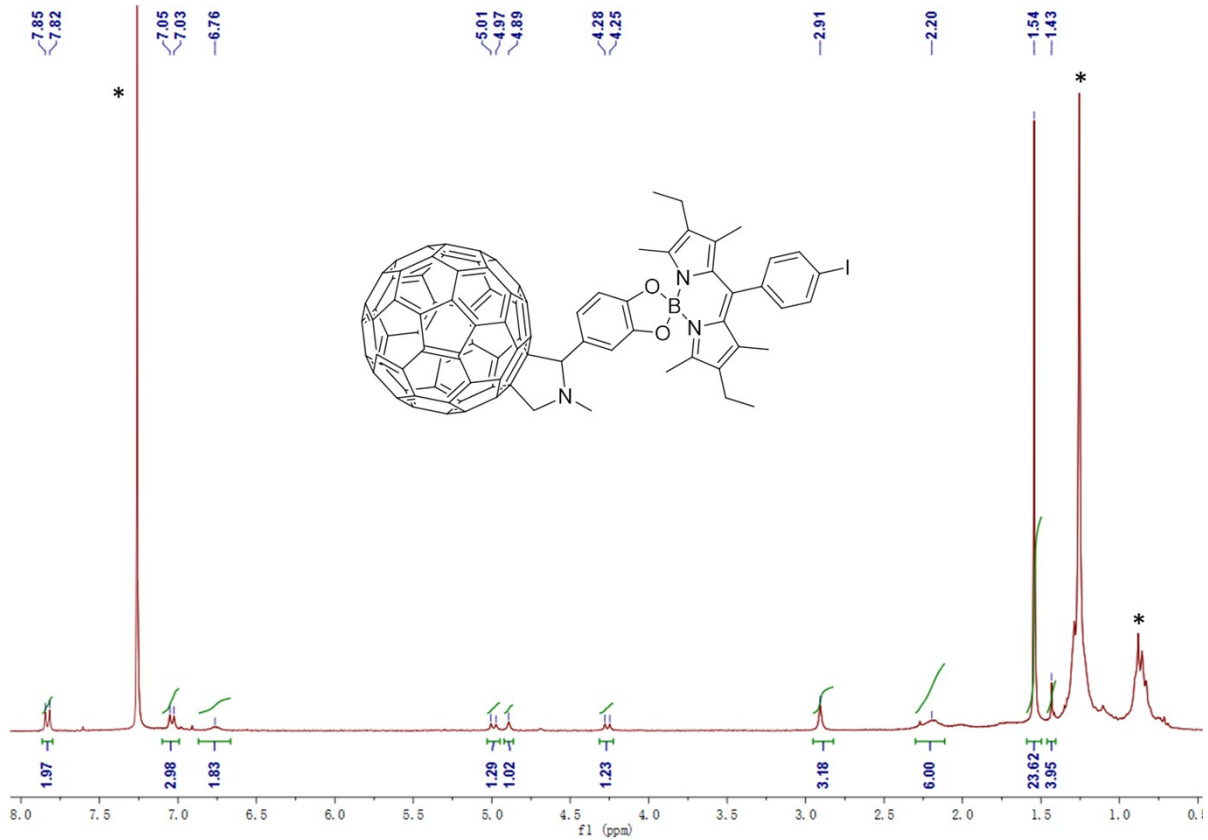


Figure S30. ^1H NMR spectra of **9** in CDCl_3 .

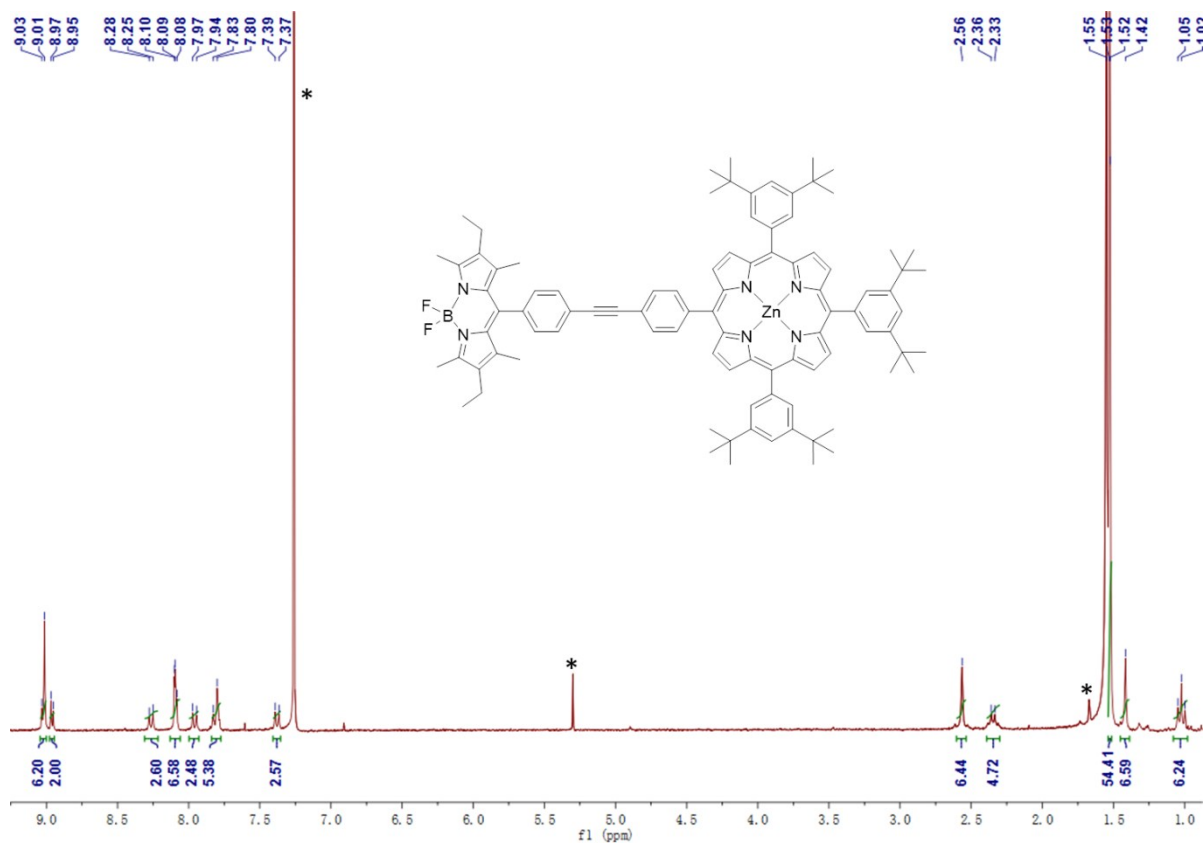


Figure S31. ^1H NMR spectra of **3** in CDCl_3 .

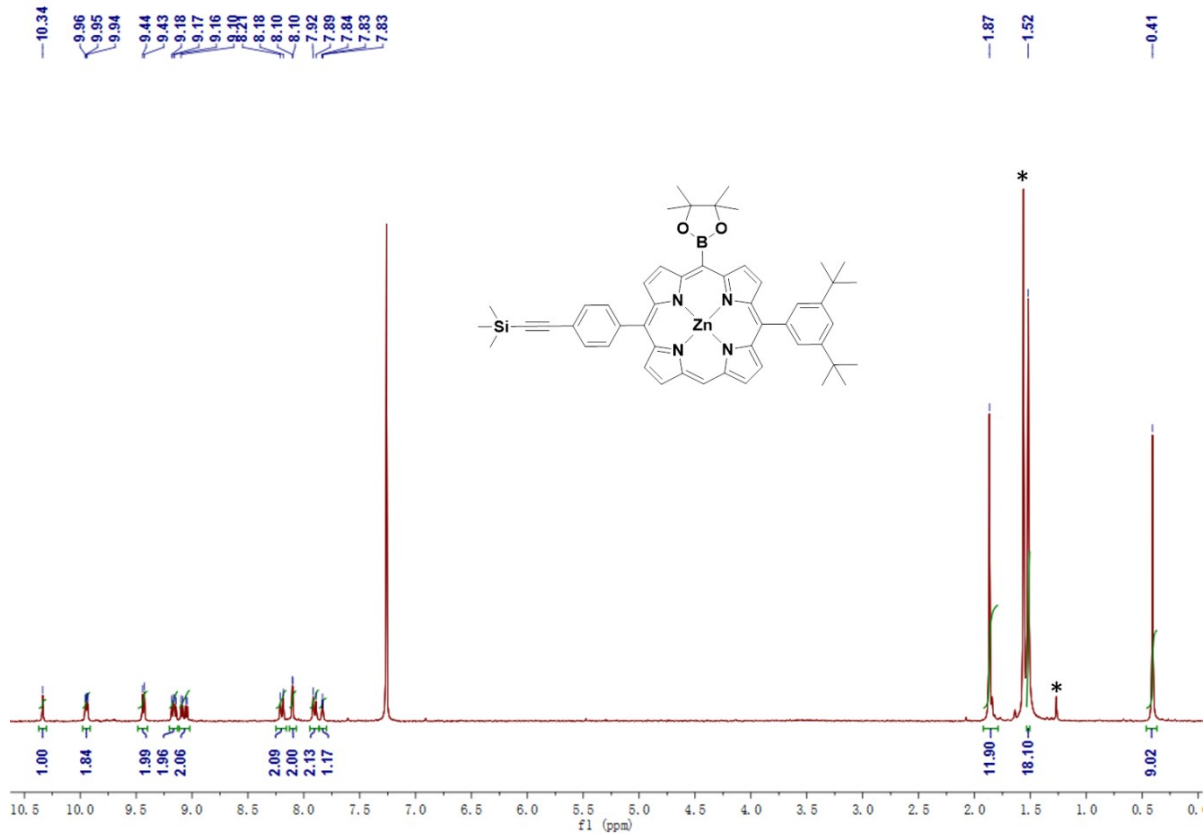


Figure S32. ^1H NMR spectra of **3** in CDCl_3 .

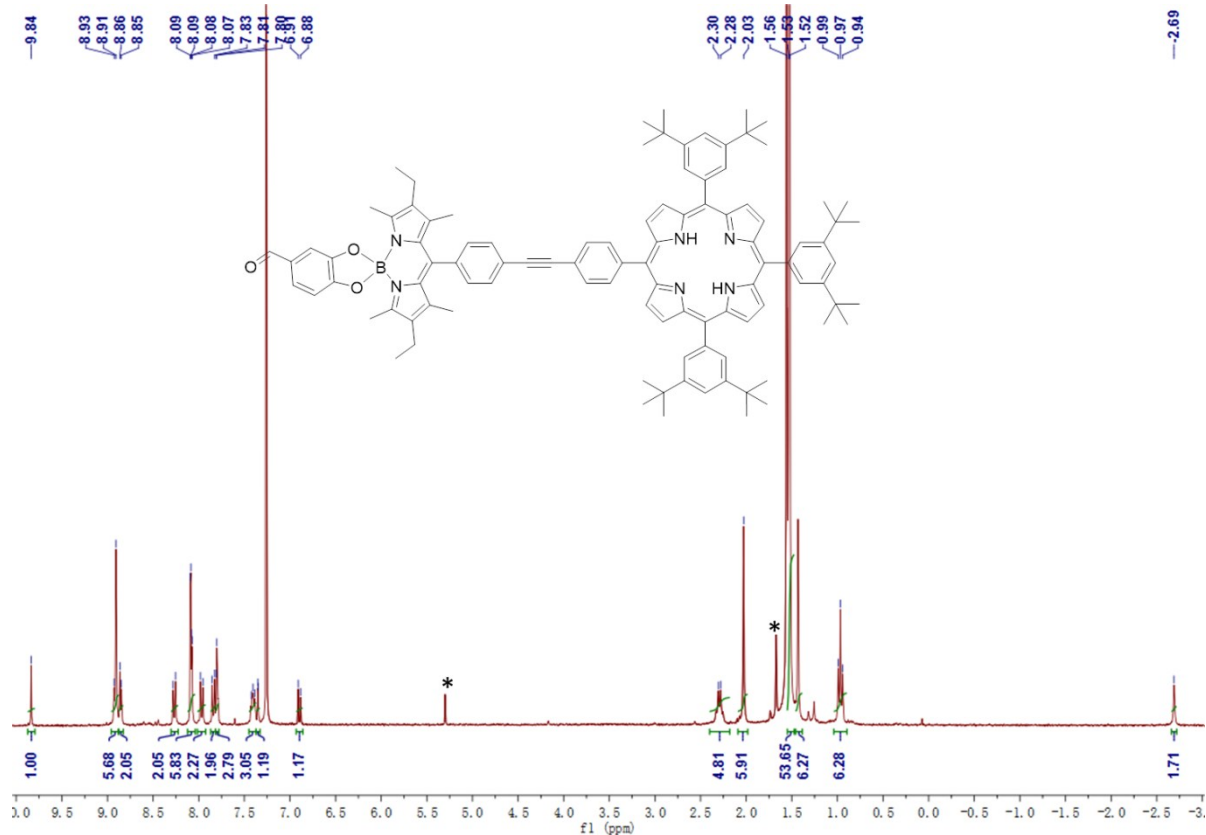


Figure S33. ^1H NMR spectra of **4** in CDCl_3 .

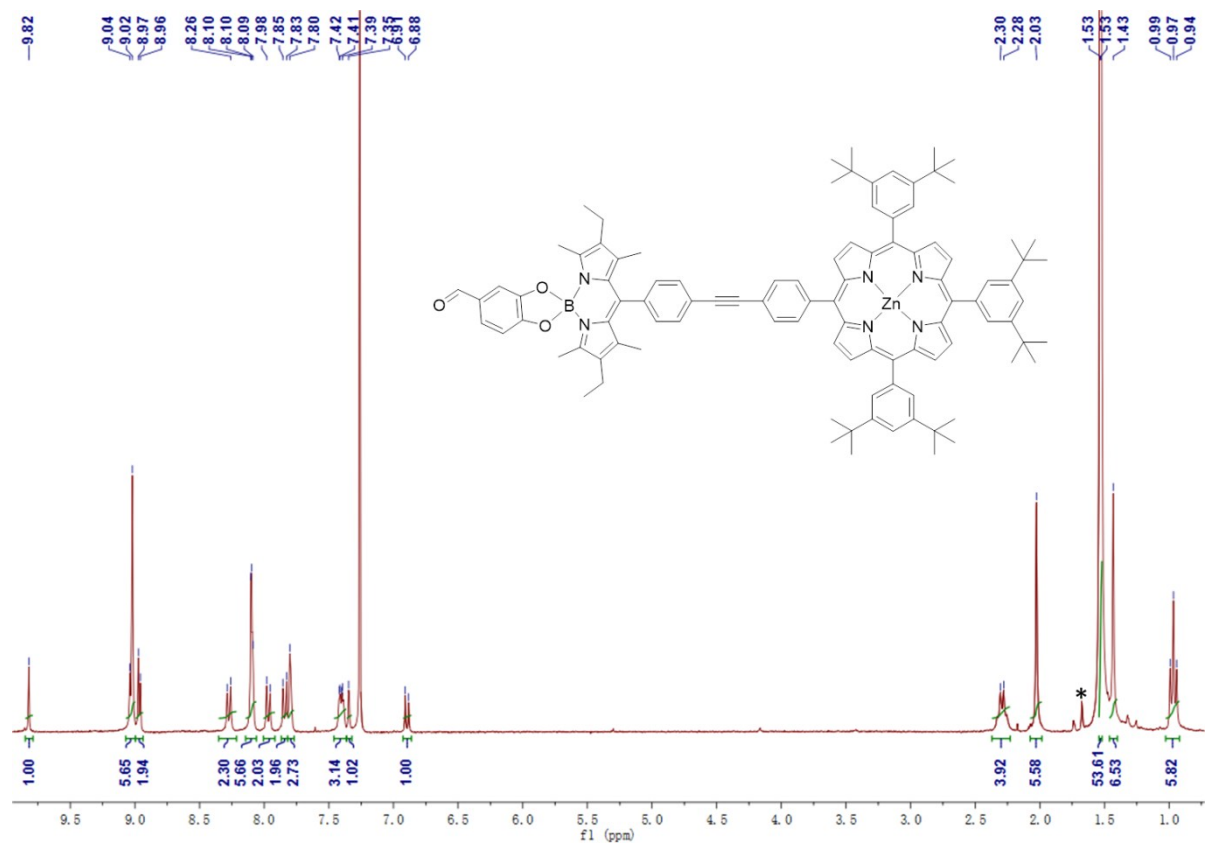


Figure S34. ^1H NMR spectra of **5** in CDCl_3 .

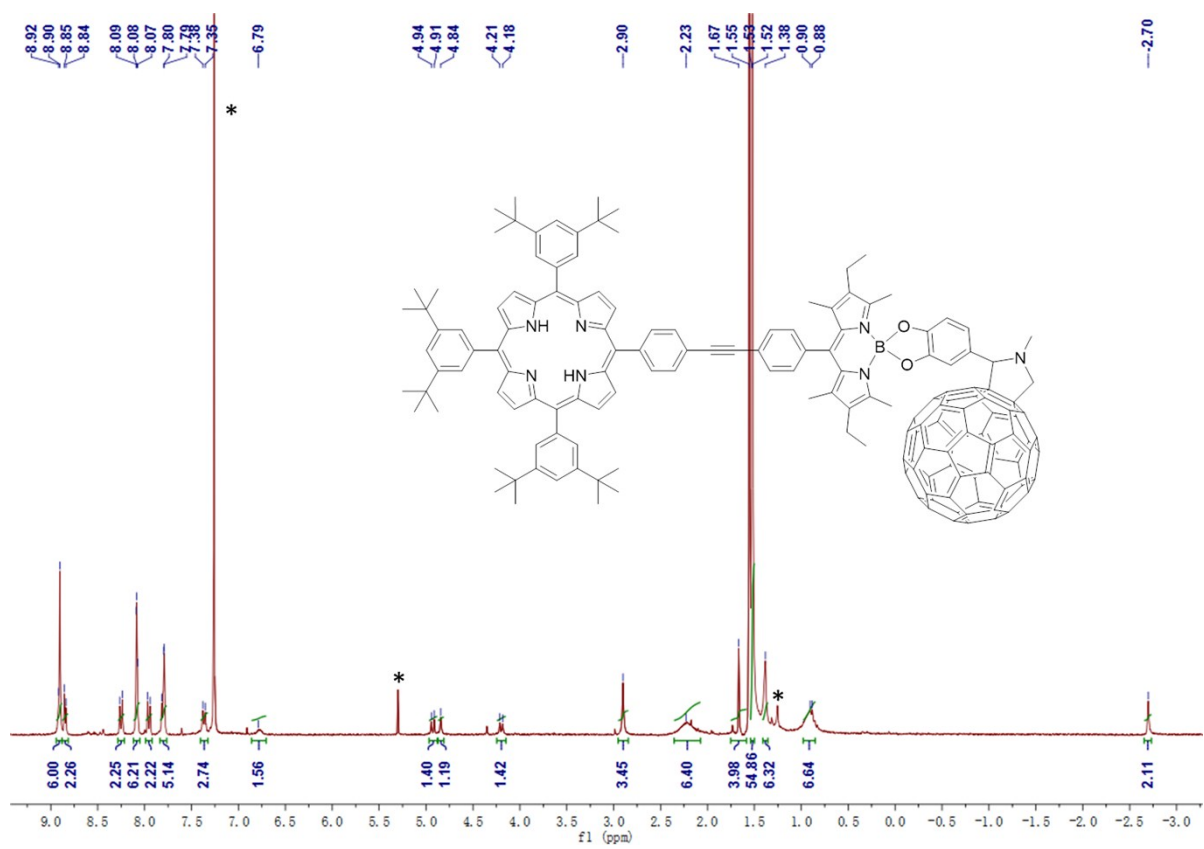


Figure S35. ^1H NMR spectra of **6** in CDCl_3 .

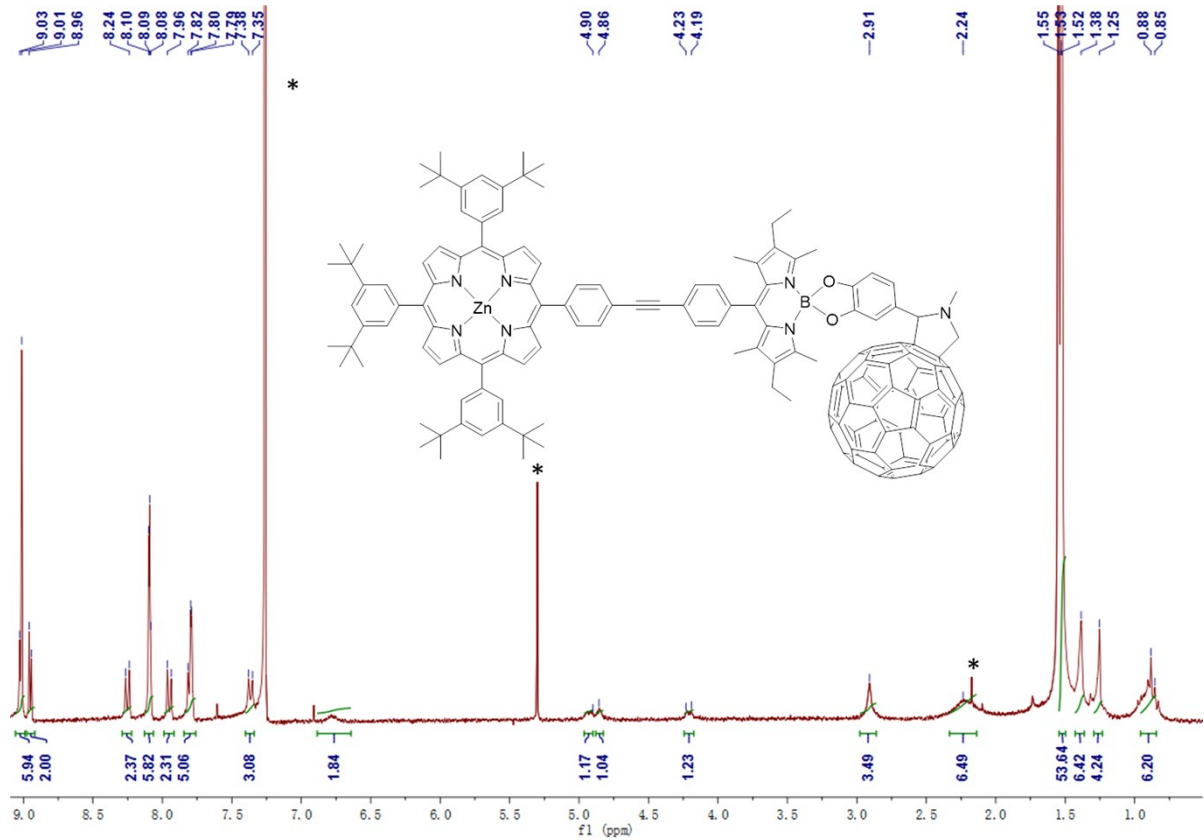


Figure S36. ^1H NMR spectra of **7** in CDCl_3 .

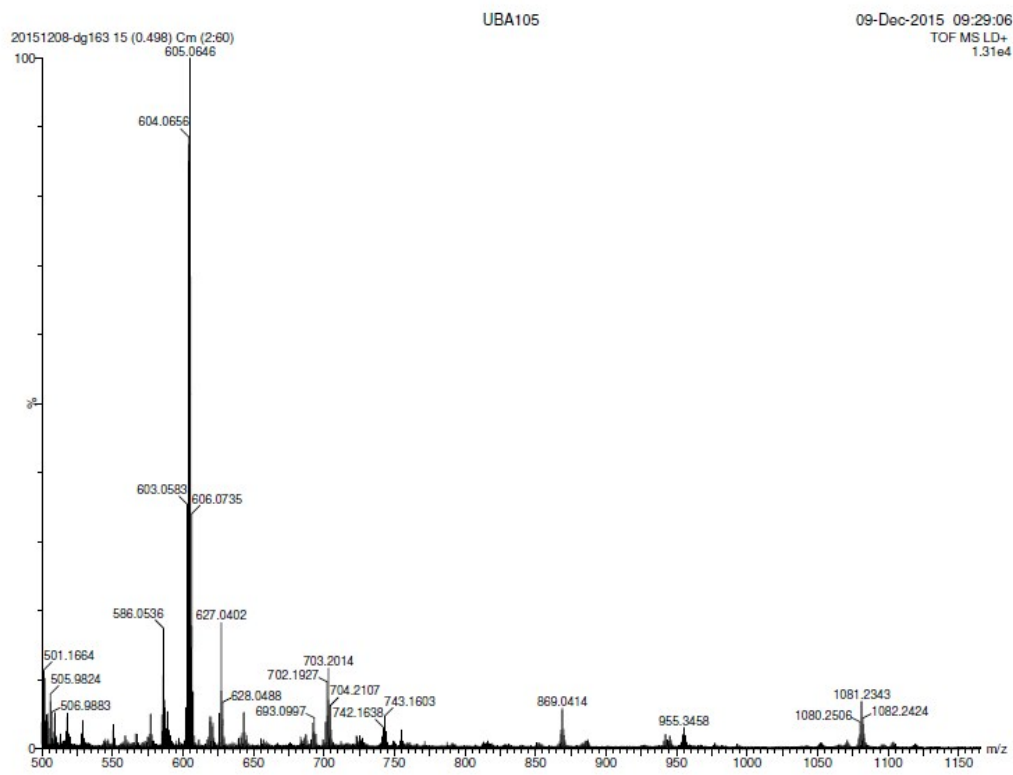


Figure S37. MALDI-TOF spectra of **8**.

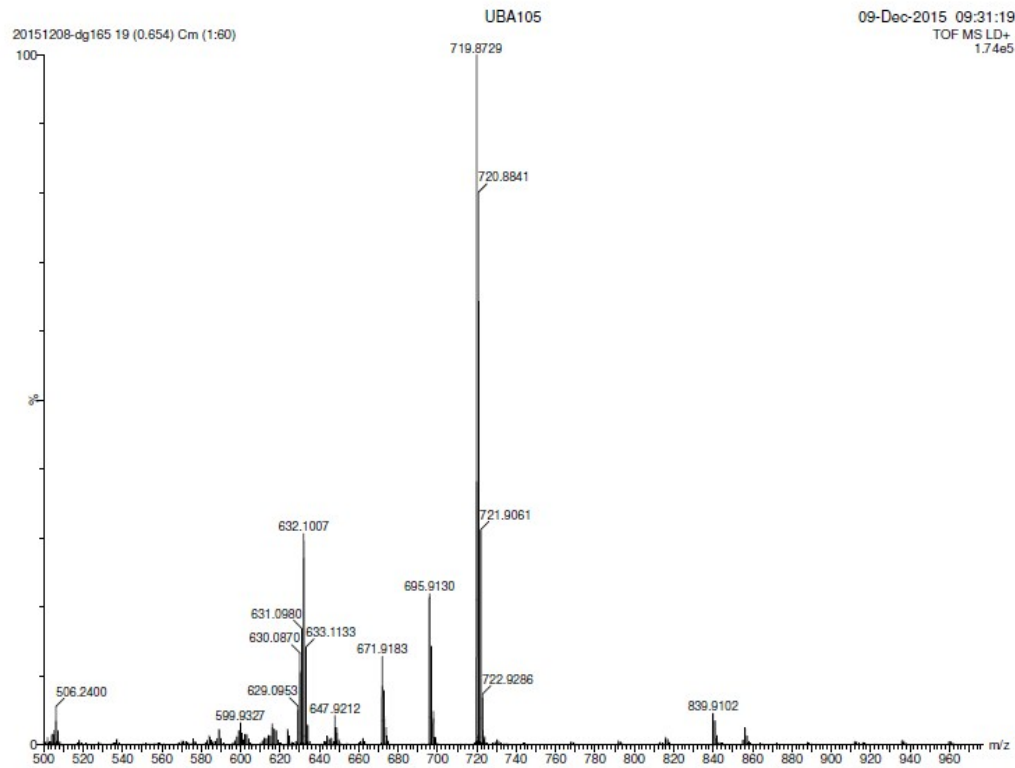


Figure S38. MALDI-TOF spectra of **9**.

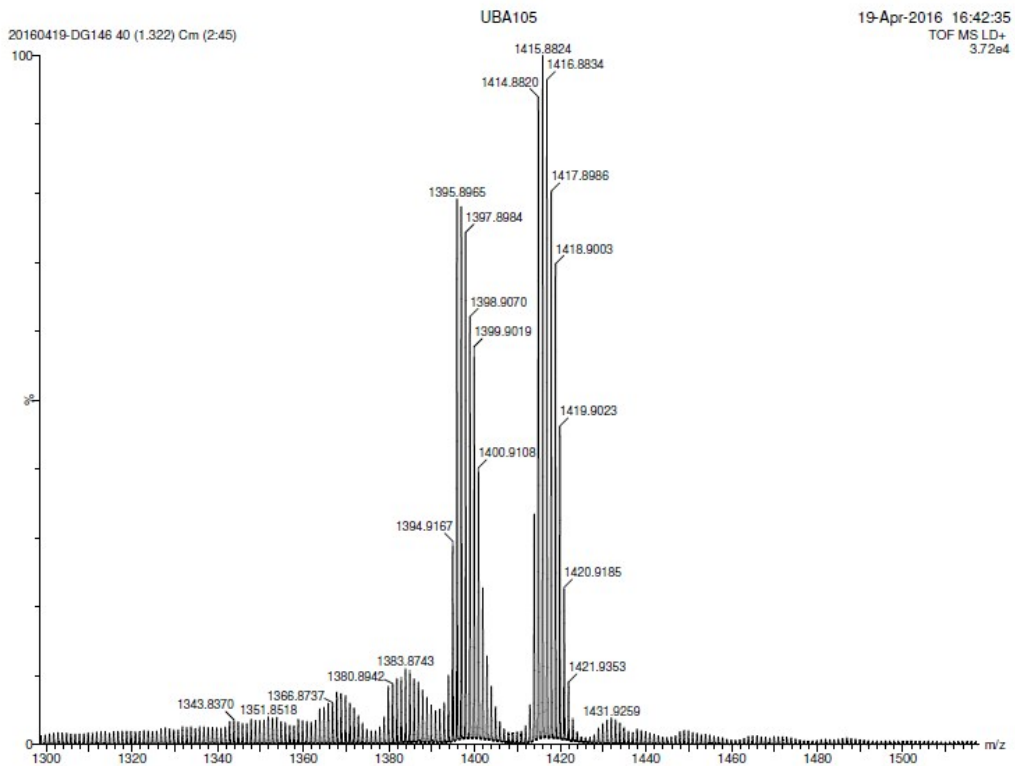


Figure S39. MALDI-TOF spectra of **3**.

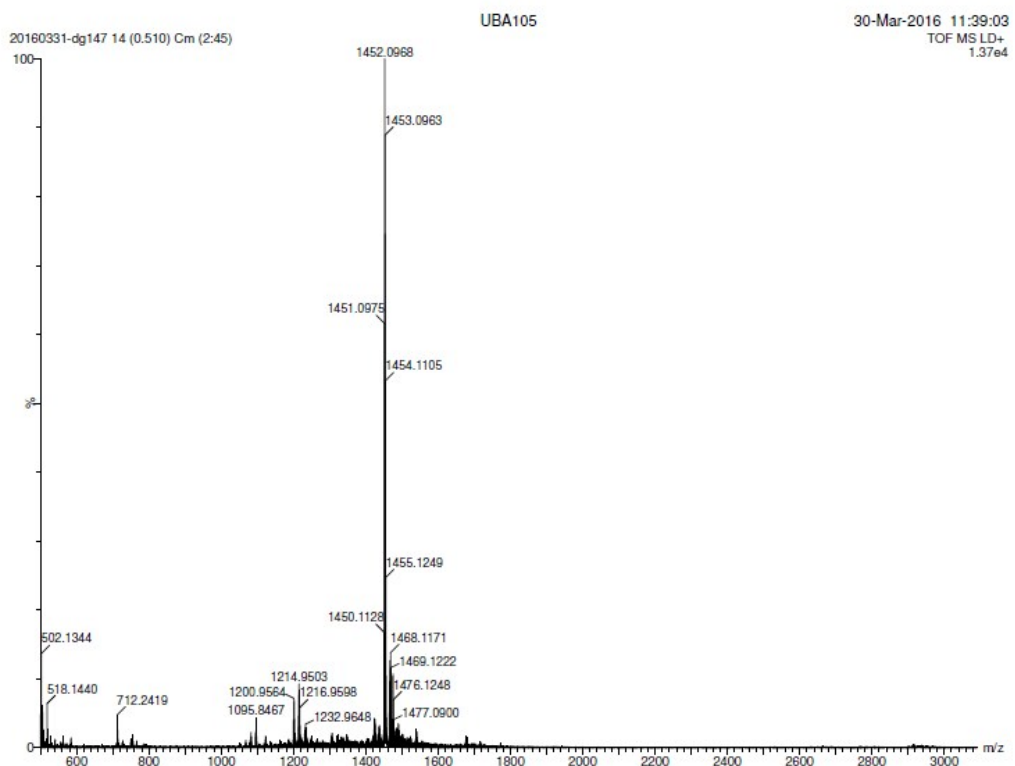


Figure S40. MALDI-TOF spectra of **4**.

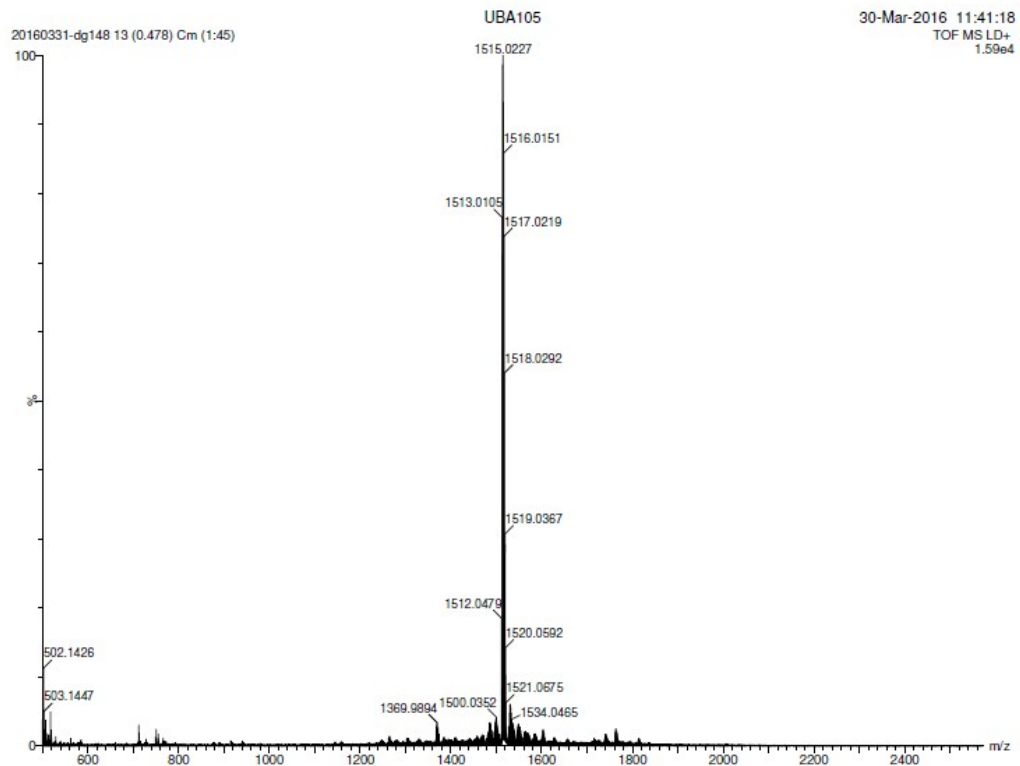


Figure S41. MALDI-TOF spectra of **5**.

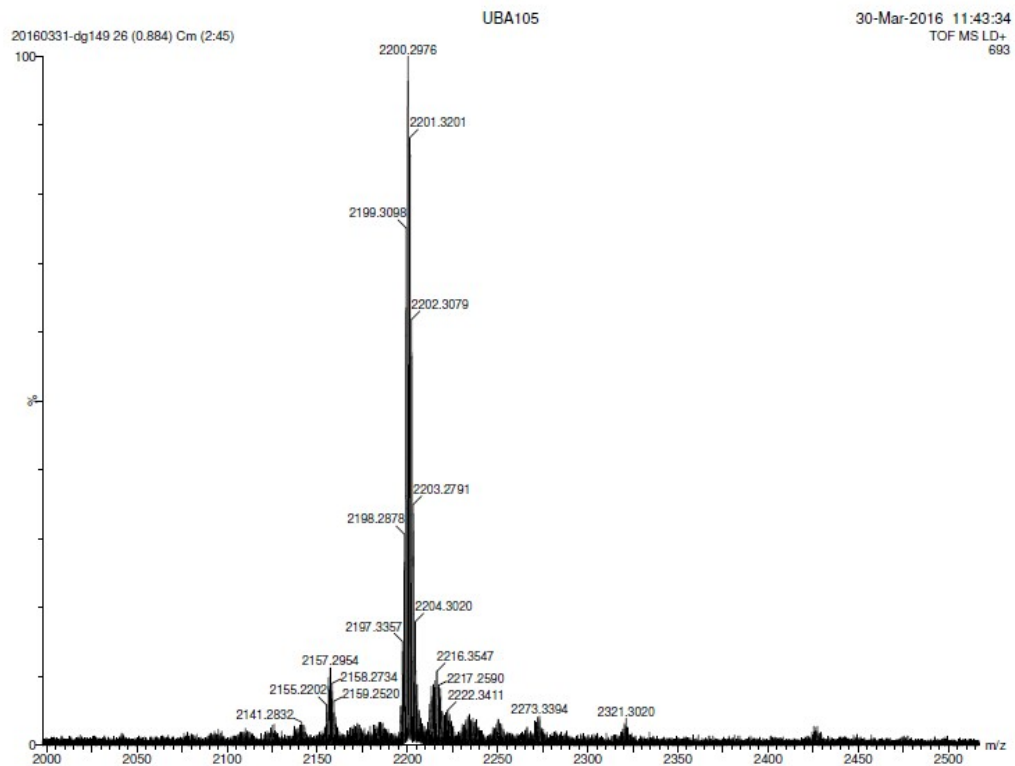


Figure S42. MALDI-TOF spectra of **6**.

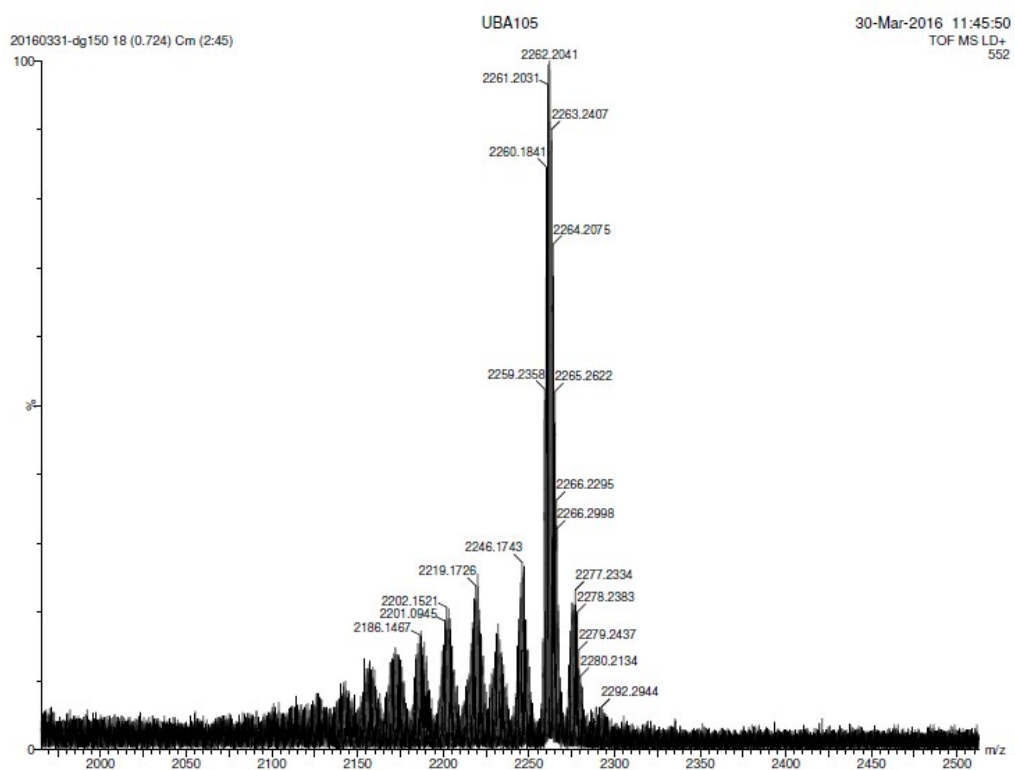


Figure S43. MALDI-TOF spectra of **7**.

Table S1. Calculated position, oscillator strength (f) and major contributions of the first 100 singlet-singlet electronic transitions for **6**.

No.	Wavelength (nm)	Osc. Strength	Major contribs (%)
1	1001.3	0.0041	H-2→LUMO (99)
2	917.7	0.0201	H-1→LUMO (99)
3	800.8	0	HOMO→LUMO (100)
4	771.2	0.0017	H-2→L+1 (97)
5	718.7	0.0002	H-1→L+1 (97)
6	701.0	0.0004	H-7→LUMO (19), H-5→LUMO (70)
7	695.6	0.0012	H-6→LUMO (88)
8	680.0	0.0006	H-7→LUMO (68), H-5→LUMO (12), H-4→LUMO (15)
9	677.1	0.0001	H-5→LUMO (11), H-4→LUMO (80)
10	670.3	0.0034	H-2→L+2 (86)
11	664.0	0	H-3→LUMO (100)
12	654.9	0	HOMO→L+1 (100)
13	636.2	0.0004	H-1→L+3 (94)
14	633.0	0.0063	H-1→L+2 (91)
15	603.8	0.0001	H-5→L+1 (89)
16	586.0	0	HOMO→L+2 (100)
17	581.9	0.0538	H-3→L+4 (16), H-3→L+5 (16), HOMO→L+4 (34), HOMO→L+5 (32)
18	579.9	0.0007	H-6→L+1 (83)
19	574.2	0.0002	H-7→L+1 (91)
20	566.2	0.0001	H-4→L+1 (96)
21	562.1	0.0037	H-10→LUMO (43), H-8→LUMO (43)
22	560.5	0	H-3→L+1 (100)
23	548.9	0.0322	HOMO→L+3 (83)
24	546.9	0.0008	H-11→LUMO (12), H-10→LUMO (48), H-8→LUMO (37)
25	544.0	0.0614	H-3→L+4 (14), H-3→L+5 (14), HOMO→L+3 (16), HOMO→L+4 (30), HOMO→L+5 (25)
26	536.9	0.0003	H-6→L+2 (87)
27	533.1	0.0006	H-5→L+2 (72)
28	525.5	0.0002	H-2→L+3 (99)
29	524.7	0.0028	H-11→LUMO (77), H-8→LUMO (16)
30	512.2	0.0001	H-4→L+2 (94)
31	511.9	0.0094	H-2→L+6 (94)
32	509.3	0	H-3→L+2 (100)
33	507.8	0.0007	H-7→L+2 (78)
34	489.2	0.0083	H-1→L+6 (98)
35	485.6	0	H-9→LUMO (99)
36	482.6	0.0021	H-10→L+1 (45), H-8→L+1 (33)
37	479.3	0.0005	H-3→L+3 (100)
38	472.4	0.0002	H-1→L+4 (99)
39	470.7	0.0022	H-18→LUMO (69), H-17→LUMO (27)
40	463.5	0	HOMO→L+6 (100)
41	463.2	0	H-1→L+5 (100)

42	462.0	0.0011	H-10→L+1 (41), H-8→L+1 (56)
43	455.5	0.0021	H-11→L+2 (12), H-10→L+2 (56), H-8→L+2 (24)
44	451.6	0	H-2→L+4 (100)
45	446.8	0.0005	H-11→L+1 (73), H-2→L+7 (13)
46	444.7	0.0034	H-11→L+1 (15), H-6→L+6 (11), H-2→L+7 (63)
47	444.1	0	H-2→L+5 (100)
48	440.8	0.2234	H-8→L+3 (17), H-5→L+3 (18), H-4→L+3 (51)
49	436.3	0	H-12→LUMO (99)
50	435.9	0.102	H-5→L+3 (64), H-4→L+3 (29)
51	429.4	0.0092	H-8→L+2 (14), H-7→L+6 (15), H-5→L+6 (51)
52	427.7	0.006	H-6→L+3 (85), H-5→L+3 (10)
53	427.5	0.0031	H-10→L+2 (23), H-8→L+2 (37), H-7→L+6 (20), H-1→L+7 (10)
54	427.3	0	H-9→L+1 (99)
55	426.9	0	H-13→LUMO (98)
56	426.5	0.0009	H-7→L+6 (33), H-6→L+6 (12), H-1→L+7 (48)
57	425.8	0.0007	H-18→LUMO (21), H-17→LUMO (51)
58	425.3	0.0022	H-17→LUMO (15), H-10→L+2 (11), H-7→L+6 (15), H-5→L+6 (27)
59	423.2	0.0094	H-4→L+4 (92)
60	422.8	0.7685	H-3→L+5 (14), HOMO→L+8 (74)
61	421.9	0.0107	H-6→L+6 (55), H-2→L+9 (13), H-1→L+7 (15)
62	418.3	0.0124	H-7→L+3 (83)
63	416.6	0.004	H-18→L+1 (37), H-17→L+1 (14), H-11→L+2 (24)
64	415.5	0.0004	H-4→L+6 (69), H-2→L+9 (10)
65	415.2	0.0225	H-8→L+3 (35), H-4→L+6 (15), H-2→L+9 (12)
66	414.9	0.0321	H-8→L+3 (25), H-4→L+6 (11), H-2→L+9 (19)
67	414.4	0.0028	H-11→L+2 (50)
68	414.1	0	H-3→L+6 (100)
69	414.1	0.0001	H-4→L+5 (100)
70	409.9	0	H-15→LUMO (21), H-14→LUMO (78)
71	408.9	0.0692	H-9→L+3 (95)
72	408.4	0	H-15→LUMO (78), H-14→LUMO (20)
73	404.3	0.0002	H-21→LUMO (94)
74	404.0	0	H-16→LUMO (95)
75	403.1	0.0002	HOMO→L+7 (100)
76	403.0	0.0007	H-24→LUMO (20), H-23→LUMO (44)
77	402.6	0.0012	H-29→LUMO (13), H-25→LUMO (13), H-24→LUMO (28)
78	401.1	0.018	H-1→L+9 (87)
79	400.6	0.0006	H-29→LUMO (11), H-25→LUMO (48), H-24→LUMO (20)
80	399.2	0.807	H-3→L+4 (41), HOMO→L+5 (19)
81	396.6	0	H-9→L+2 (99)
82	394.7	0	H-19→LUMO (100)
83	394.3	0.0042	H-29→LUMO (13), H-26→LUMO (36), H-23→LUMO (19)
84	393.2	0.0035	H-1→L+8 (98)
85	391.4	0.0007	H-23→LUMO (10), H-18→L+2 (40), H-17→L+2 (15)
86	389.6	0.0139	H-30→LUMO (66), H-25→LUMO (13)

87	389.0	0	H-12→L+1 (99)
88	388.4	1.234	H-9→L+4 (16), H-3→L+4 (10), H-3→L+5 (29), HOMO→L+4 (13), HOMO→L+8 (13)
89	385.9	0.0048	H-27→LUMO (70)
90	385.9	0	H-20→LUMO (99)
91	384.0	0.0002	H-5→L+4 (100)
92	383.5	0.0056	H-29→LUMO (20), H-26→LUMO (15), H-23→L+1 (19), H-5→L+7 (11)
93	381.6	0	H-13→L+1 (99)
94	379.3	0	H-6→L+4 (100)
95	378.7	0.0009	H-18→L+1 (21), H-17→L+1 (48), H-6→L+7 (16)
96	378.5	0	H-5→L+5 (100)
97	378.2	0.0041	H-12→L+4 (48), H-12→L+5 (39)
98	377.8	0.0007	H-17→L+1 (16), H-6→L+7 (46)
99	377.2	0	H-22→LUMO (99)
100	376.0	0	HOMO→L+9 (100)

Table S2. Calculated position, oscillator strength (f) and major contributions of the first 100 singlet-singlet electronic transitions for **7**.

No.	Wavelength (nm)	Osc. Strength	Major contribs (%)
1	1002.4	0.0036	H-2→LUMO (97)
2	923.4	0.0185	H-1→LUMO (97)
3	771.8	0.0016	H-2→L+1 (96)
4	766.0	0	HOMO→LUMO (100)
5	722.3	0.0005	H-1→L+1 (97)
6	700.7	0.0004	H-7→LUMO (19), H-5→LUMO (71)
7	695.6	0.0012	H-6→LUMO (88)
8	689.4	0	H-3→LUMO (100)
9	688.7	0.0007	H-4→LUMO (90)
10	679.5	0.0004	H-7→LUMO (67), H-5→LUMO (22)
11	670.1	0.0034	H-2→L+2 (89)
12	635.7	0.0068	H-1→L+2 (97)
13	632.1	0.0001	H-1→L+3 (99)
14	631.8	0	HOMO→L+1 (100)
15	603.9	0.0001	H-5→L+1 (89)
16	580.2	0.0009	H-6→L+1 (81)
17	578.8	0	H-3→L+1 (100)
18	574.6	0.0002	H-7→L+1 (83)
19	573.8	0	H-4→L+1 (89)
20	567.3	0	HOMO→L+2 (100)
21	563.0	0.0036	H-10→LUMO (38), H-8→LUMO (45)
22	549.5	0.001	H-10→LUMO (54), H-8→LUMO (32)
23	541.1	0.0548	H-3→L+5 (38), HOMO→L+4 (60)
24	538.9	0.0147	H-3→L+4 (41), HOMO→L+5 (57)
25	536.8	0.0003	H-6→L+2 (86)
26	533.1	0.0005	H-6→L+2 (10), H-5→L+2 (72)
27	526.1	0.0011	HOMO→L+3 (98)
28	525.8	0.0024	H-11→LUMO (81), H-8→LUMO (12)
29	524.2	0	H-3→L+2 (100)
30	522.4	0.0015	H-2→L+3 (99)
31	517.9	0	H-4→L+2 (98)
32	512.2	0.0087	H-2→L+6 (95)
33	508.2	0.0008	H-7→L+2 (81)
34	490.7	0.0013	H-9→LUMO (83), H-1→L+6 (11)
35	490.6	0.0065	H-9→LUMO (11), H-1→L+6 (86)
36	487.8	0.0001	H-3→L+3 (100)
37	483.2	0.0022	H-10→L+1 (44), H-8→L+1 (32)
38	470.8	0.0021	H-19→LUMO (84), H-17→LUMO (12)
39	464.5	0.0011	H-10→L+1 (41), H-8→L+1 (53)
40	459.5	0.0002	H-1→L+4 (99)
41	455.6	0.0021	H-11→L+2 (12), H-10→L+2 (57), H-8→L+2 (21)
42	452.0	0	H-1→L+5 (100)

43	451.8	0	HOMO→L+6 (100)
44	447.3	0.0005	H-11→L+1 (80)
45	444.6	0.0036	H-6→L+6 (12), H-2→L+7 (70)
46	439.8	0.0006	H-2→L+4 (100)
47	439.7	0.2549	H-8→L+3 (15), H-5→L+3 (12), H-4→L+3 (60)
48	434.3	0.0817	H-5→L+3 (70), H-4→L+3 (22)
49	433.8	0	H-2→L+5 (100)
50	431.5	0	H-9→L+1 (93)
51	430.2	0.0067	H-10→L+2 (11), H-8→L+2 (43), H-5→L+6 (29)
52	429.1	0.0021	H-17→LUMO (35), H-7→L+6 (10), H-1→L+7 (15)
53	428.2	0.0004	H-17→LUMO (46), H-7→L+6 (13), H-1→L+7 (13)
54	427.2	0.0004	H-7→L+6 (36), H-1→L+7 (47)
55	425.8	0.0048	H-7→L+6 (26), H-5→L+6 (39)
56	425.6	0.008	H-6→L+3 (84), H-5→L+3 (11)
57	424.0	0	H-3→L+6 (100)
58	422.1	0.0102	H-6→L+6 (60), H-2→L+9 (12), H-1→L+7 (10)
59	420.9	0	H-12→LUMO (99)
60	419.3	0.0002	H-4→L+6 (96)
61	417.1	0.0133	H-8→L+3 (25), H-7→L+3 (45), H-4→L+4 (14)
62	416.9	0.0113	H-19→L+1 (40), H-11→L+2 (29)
63	415.8	0.0011	H-7→L+3 (34), H-4→L+4 (60)
64	415.3	0.0042	H-19→L+1 (19), H-11→L+2 (13), H-2→L+9 (30)
65	414.8	0.0179	H-11→L+2 (38), H-2→L+9 (21)
66	414.4	0.045	H-8→L+3 (40), H-7→L+3 (19), H-4→L+4 (18)
67	413.8	0	H-13→LUMO (98)
68	413.4	0.8502	H-3→L+5 (14), HOMO→L+4 (11), HOMO→L+8 (66)
69	411.5	0	H-14→LUMO (99)
70	409.5	0.0004	H-9→L+3 (87)
71	407.7	0	H-4→L+5 (100)
72	406.6	0.0001	H-23→LUMO (97)
73	405.6	0	H-15→LUMO (99)
74	403.2	0	H-16→LUMO (100)
75	403.1	0.0002	H-27→LUMO (21), H-26→LUMO (33), H-1→L+9 (19)
76	402.7	0.0028	H-31→LUMO (15), H-28→LUMO (11), H-27→LUMO (15), H-26→LUMO (21), H-1→L+9 (10)
77	402.1	0.0125	H-27→LUMO (16), H-1→L+9 (67)
78	400.6	0.0003	H-31→LUMO (10), H-28→LUMO (52), H-27→LUMO (16)
79	400.0	0	H-9→L+2 (93)
80	398.9	0	H-18→LUMO (99)
81	394.4	0.003	H-31→LUMO (13), H-29→LUMO (36), H-26→LUMO (19)
82	394.0	0	HOMO→L+7 (100)
83	393.3	0.673	H-3→L+4 (37), H-3→L+8 (37), HOMO→L+5 (23)
84	392.9	0	H-21→LUMO (12), H-20→LUMO (87)
85	392.8	0.0019	H-1→L+8 (99)
86	391.4	0.0009	H-26→LUMO (10), H-19→L+2 (49)

87	390.9	0	H-21→LUMO (86), H-20→LUMO (13)
88	389.7	0.007	H-32→LUMO (65), H-28→LUMO (13)
89	387.7	0	H-22→LUMO (98)
90	386.0	0.0876	H-30→LUMO (67)
91	385.3	1.2232	H-9→L+4 (16), H-3→L+5 (33), HOMO→L+4 (19), HOMO→L+8 (23)
92	383.8	0.0062	H-31→LUMO (18), H-29→LUMO (14), H-26→L+1 (18), H-17→L+1 (11), H-5→L+7 (10)
93	380.7	0.0017	H-19→L+1 (11), H-17→L+1 (69)
94	380.3	0	H-24→LUMO (99)
95	377.9	0.0007	H-6→L+7 (60)
96	376.9	0	H-12→L+1 (99)
97	376.6	0.6628	H-3→L+4 (17), H-3→L+8 (60), HOMO→L+5 (16)
98	375.9	0.0056	H-26→L+1 (11), H-5→L+7 (49)
99	375.5	0.0003	H-5→L+4 (89), H-4→L+8 (10)
100	375.0	0.0012	H-5→L+4 (11), H-4→L+8 (81)